



**MADE3 – description  
and test**

J. C. Kaiser et al.

Title Page

Abstract

Introduction

Conclusions

References

Tables

Figures

◀

▶

◀

▶

Back

Close

Full Screen / Esc

Printer-friendly Version

Interactive Discussion



This discussion paper is/has been under review for the journal Geoscientific Model Development (GMD). Please refer to the corresponding final paper in GMD if available.

# The MESSy aerosol submodel MADE3 (v2.0b): description and a box model test

J. C. Kaiser<sup>1</sup>, J. Hendricks<sup>1</sup>, M. Righi<sup>1</sup>, N. Riemer<sup>2</sup>, R. A. Zaveri<sup>3</sup>, S. Metzger<sup>4,5</sup>,  
and V. Aquila<sup>6</sup>

<sup>1</sup>Deutsches Zentrum für Luft- und Raumfahrt (DLR), Institut für Physik der Atmosphäre, Oberpfaffenhofen, Germany

<sup>2</sup>Department of Atmospheric Sciences, University of Illinois at Urbana-Champaign, Urbana, IL, USA

<sup>3</sup>Atmospheric Sciences and Global Change Division, Pacific Northwest National Laboratory, Richland, WA 99352, USA

<sup>4</sup>The Cyprus Institute, Nicosia, Cyprus

<sup>5</sup>Max Planck Institute for Chemistry, Mainz, Germany

<sup>6</sup>GESTAR/Johns Hopkins University, Department of Earth and Planetary Sciences, Johns Hopkins University, Baltimore, MD, USA

Received: 13 December 2013 – Accepted: 8 January 2014 – Published: 21 January 2014

Correspondence to: J. C. Kaiser (christopher.kaiser@dlr.de)

Published by Copernicus Publications on behalf of the European Geosciences Union.

## Abstract

We introduce MADE3 (Modal Aerosol Dynamics model for Europe, adapted for global applications, 3rd generation), an aerosol dynamics submodel for application within the MESSy framework (Modular Earth Submodel System). MADE3 builds on the predecessor aerosol submodels MADE and MADE-in. Its main new features are the explicit representation of coarse particle interactions both with other particles and with condensable gases, and the inclusion of hydrochloric acid (HCl)/chloride (Cl) partitioning between the gas and condensed phases. The aerosol size distribution is represented in the new submodel as a superposition of nine lognormal modes: one for fully soluble particles, one for insoluble particles, and one for mixed particles in each of three size ranges (Aitken, accumulation, and coarse mode size ranges).

In order to assess the performance of MADE3 we compare it to its predecessor MADE and to the much more detailed particle-resolved aerosol model PartMC-MOSAIC in a box model simulation of an idealised marine boundary layer test case. MADE3 and MADE results are very similar, except in the coarse mode, where the aerosol is dominated by sea spray particles. Cl is reduced in MADE3 with respect to MADE due to the HCl/Cl partitioning that leads to Cl removal from the sea spray aerosol in our test case. Additionally, aerosol nitrate concentration is higher in MADE3 due to the condensation of nitric acid on coarse particles. MADE3 and PartMC-MOSAIC show substantial differences in the fine particle size distributions (sizes  $\lesssim 2\mu\text{m}$ ) that could be relevant when simulating climate effects on a global scale. Nevertheless, the agreement between MADE3 and PartMC-MOSAIC is very good when it comes to coarse particle size distribution, and also in terms of aerosol composition. Considering these results and the well-established ability of MADE in reproducing observed aerosol loadings and composition, MADE3 seems suitable for application within a global model.

GMDD

7, 691–739, 2014

## MADE3 – description and test

J. C. Kaiser et al.

Title Page

Abstract

Introduction

Conclusions

References

Tables

Figures

◀

▶

◀

▶

Back

Close

Full Screen / Esc

Printer-friendly Version

Interactive Discussion



## 1 Introduction

Aerosol particles affect the energy balance of the earth both directly by scattering or absorbing radiation and indirectly by acting as cloud condensation nuclei. The present-day net effect of these processes is probably a negative radiative forcing (RF) with respect to preindustrial times (e.g. Forster et al., 2007; Bellouin et al., 2013; Naik et al., 2013). Hence, the concurrent positive forcing by long-lived greenhouse gases may be partly offset by the aerosol forcing.

Global model simulations have indicated that the emissions from ocean ship traffic may be one of the largest contributors to the anthropogenic aerosol forcing (Lauer et al., 2007, 2009; Righi et al., 2011, 2013; Olivie' et al., 2012; Peters et al., 2012, 2013). That contribution is mainly caused by the sulfur in the ship exhaust plumes that leads to the formation of aerosol sulfate ( $\text{SO}_4$ ). Both nucleation of new particles and condensation of sulfuric acid ( $\text{H}_2\text{SO}_4$ ) on emitted as well as on background particles contribute to  $\text{SO}_4$  formation.

The International Maritime Organization (IMO) has set limits on allowed shipping fuel sulfur content that will be further tightened in the future (IMO, 2011) in order to improve air quality in port cities and along coasts. On the one hand, the sulfur reduction leads to a decrease of aerosol  $\text{SO}_4$  concentrations (Lauer et al., 2009; Righi et al., 2011; Johansson et al., 2013). On the other hand, the reduced  $\text{SO}_4$  concentrations allow more aerosol nitrate ( $\text{NO}_3$ ) formation by condensation of nitric acid ( $\text{HNO}_3$ ). Increased nitrate content was shown to make up for a substantial fraction of the  $\text{SO}_4$  reduction (Lauer et al., 2009; Bellouin et al., 2011; Righi et al., 2011). The aerosol RF and total particulate mass concentrations may therefore not be reduced as much as the  $\text{SO}_4$  concentrations.

A number of measurements suggest that aerosol  $\text{NO}_3$  may primarily partition to the coarse mode both under clean marine conditions and when marine aerosol is affected by anthropogenic pollution (Kerminen et al., 1997; Hara et al., 1999; Yeatman et al., 2001; Cavalli et al., 2004; Nolte et al., 2008). However, in the assessment of the ship

GMDD

7, 691–739, 2014

### MADE3 – description and test

J. C. Kaiser et al.

Title Page

Abstract

Introduction

Conclusions

References

Tables

Figures

◀

▶

◀

▶

Back

Close

Full Screen / Esc

Printer-friendly Version

Interactive Discussion



emissions' effects on climate by Peters et al. (2012, 2013), NO<sub>3</sub> formation was not included at all, and the low-sulfur shipping fuel studies by Lauer et al. (2009) and Righi et al. (2011) did not include interactions of condensable gases with coarse particles (except for water vapour). These deficiencies may have led to errors in the quantification of low-sulfur fuel effects.

To improve on the previous investigations, we developed MADE3 for use within the MESSy framework (Jöckel et al., 2005, 2010). Via this framework, MADE3 can be coupled to an atmospheric chemistry scheme and to the general circulation model ECHAM5 (Roeckner et al., 2006), which together form the atmospheric chemistry general circulation model (AC-GCM) EMAC (ECHAM5/MESSy2 atmospheric chemistry model). MADE3 is based on MADE (Ackermann et al., 1998; Lauer et al., 2005) and MADE-in (Aquila et al., 2011), but for the first time includes interactions of coarse particles with both condensable gases and other particles. To enable the further extension we restructured and improved major parts of the submodel code. Our main motivation for the development of MADE3 is a reassessment of the aerosol perturbations caused by global ship traffic under current and future scenarios for fuel sulfur content.

Some essential processes, e.g. particle transport and deposition, are not included in MADE3 because they are treated by other submodels within the MESSy framework. It is therefore not feasible to evaluate a stand-alone (box model) setup of MADE3 by comparison with measured data. Instead, we test here the algorithms used in MADE3 for solving the aerosol microphysics equations. In order to assess improvements, strengths, and weaknesses of the new submodel, we compare it to its predecessor MADE and to the particle-resolved stand-alone aerosol model PartMC-MOSAIC (Riemer et al., 2009; Zaveri et al., 2008) in a box model application. For that purpose we define a marine background setup with added emissions representative of heavy ship traffic. We use MADE for comparison because previous studies on the shipping effect were carried out with this submodel (Lauer et al., 2007, 2009; Righi et al., 2011, 2013). PartMC-MOSAIC is regarded as a reference to test how well MADE3 performs as

**MADE3 – description and test**

J. C. Kaiser et al.

[Title Page](#)[Abstract](#)[Introduction](#)[Conclusions](#)[References](#)[Tables](#)[Figures](#)[◀](#)[▶](#)[◀](#)[▶](#)[Back](#)[Close](#)[Full Screen / Esc](#)[Printer-friendly Version](#)[Interactive Discussion](#)

a solver for the aerosol dynamics equation. Implementation and evaluation of MADE3 within EMAC will be the subject of a follow-up study.

This paper is organised as follows: in Sect. 2 we first describe the new submodel MADE3 in detail, then briefly state the most important improvements with respect to its predecessor MADE, and finally summarise the main features of PartMC-MOSAIC with a focus on the differences to MADE3. Section 3 contains the definition of our marine boundary layer test case. We report and discuss the results of the simulations with this setup in Sect. 4. Finally, in Sect. 5, we summarise our findings and present the conclusions.

## 2 Model description

We use the term “aerosol (sub)model” here to refer to the computer code used to solve the aerosol dynamics equation. Generally speaking, aerosol dynamics includes emissions, gas-to-particle conversion, transport, physical and chemical processing, and deposition of particles. Throughout this paper we focus on internal processes, i.e. those that are actually calculated by the aerosol submodel MADE3. These processes include gas-particle partitioning of semi-volatile species, condensation of nonvolatile  $\text{H}_2\text{SO}_4$ , formation of secondary organics, new particle formation by nucleation, as well as intra- and intermodal coagulation. We add emissions in order to test the reaction of the internal processes to external perturbations. Transport and loss processes are excluded because they are treated by other submodels within the MESSy framework.

### MADE3 – description and test

J. C. Kaiser et al.

Title Page

Abstract

Introduction

Conclusions

References

Tables

Figures

◀

▶

◀

▶

Back

Close

Full Screen / Esc

Printer-friendly Version

Interactive Discussion



The aerosol dynamics equation thus takes on the following general form (nomenclature based on Riemer et al., 2009):

$$\begin{aligned}
 \frac{\partial n^*(\boldsymbol{\mu}, t)}{\partial t} = & \underbrace{\frac{1}{2} \int_0^{\mu_1} \int_0^{\mu_2} \dots \int_0^{\mu_A} K(\boldsymbol{\mu}', \boldsymbol{\mu} - \boldsymbol{\mu}') n^*(\boldsymbol{\mu}', t) n^*(\boldsymbol{\mu} - \boldsymbol{\mu}', t) d\mu'_1 d\mu'_2 \dots d\mu'_A}_{\text{coagulation gain}} \\
 & - \underbrace{\int_0^{\infty} \int_0^{\infty} \dots \int_0^{\infty} K(\boldsymbol{\mu}, \boldsymbol{\mu}') n^*(\boldsymbol{\mu}, t) n^*(\boldsymbol{\mu}', t) d\mu'_1 d\mu'_2 \dots d\mu'_A}_{\text{coagulation loss}} \\
 & - \underbrace{\sum_{i=1}^C \frac{\partial}{\partial \mu_i} (I_i(\boldsymbol{\mu}, \mathbf{g}, t) n^*(\boldsymbol{\mu}, t))}_{\text{condensation/evaporation}} - \underbrace{\frac{\partial}{\partial \mu_{C+1}} (I_w(\boldsymbol{\mu}, \mathbf{g}, t) n^*(\boldsymbol{\mu}, t))}_{\text{water transfer}} \\
 & + \underbrace{\dot{n}^*_{\text{nuc}}(\boldsymbol{\mu}, t)}_{\text{nucleation}} + \underbrace{\dot{n}^*_{\text{emit}}(\boldsymbol{\mu}, t)}_{\text{emission}}
 \end{aligned} \tag{1}$$

- 5 Each aerosol particle is described by a vector  $\boldsymbol{\mu}$  composed of the masses  $\mu_a$  of the species  $a = 1, \dots, A$ . The number distribution of these particles (defined in the  $A$ -dimensional “species space”) is given by

$$n^*(\boldsymbol{\mu}, t) = \frac{\partial^A N^*(\boldsymbol{\mu}, t)}{\partial \mu_1 \partial \mu_2 \dots \partial \mu_A} \tag{2}$$

- 10 where  $N^*(\boldsymbol{\mu}, t)$  is the cumulative number concentration of particles containing less than the mass  $\mu_a$  of species  $a$ . The two coagulation terms (i.e. gain and loss) are calculated based on the collision probability  $K(\boldsymbol{\mu}_1, \boldsymbol{\mu}_2)$  of particles described by the vectors  $\boldsymbol{\mu}_1$  and  $\boldsymbol{\mu}_2$ . The per-particle flux of condensable gases between the gas and the condensed

MADE3 – description  
and test

J. C. Kaiser et al.

Title Page

Abstract

Introduction

Conclusions

References

Tables

Figures

◀

▶

◀

▶

Back

Close

Full Screen / Esc

Printer-friendly Version

Interactive Discussion



phase is  $I_i(\boldsymbol{\mu}, \mathbf{g}, t)$  where  $i = w$  stands for water vapour and the vector  $\mathbf{g}$  describes the gas composition. The components of the gas phase vector are the concentrations  $g_i$  of the  $i = 1, \dots, G$  different gas species. Condensable gases, i.e. the ones considered here, are assumed to be the first  $i = 1, \dots, C$  of these species and correspond to the first  $a = 1, \dots, C$  aerosol species. The species  $C + 1$  is assumed to be water vapour or liquid water, respectively. The number distribution production rates  $\dot{n}_{\text{nuc}}^*(\boldsymbol{\mu}, t)$  and  $\dot{n}_{\text{emit}}^*(\boldsymbol{\mu}, t)$  describe the addition of new particles by nucleation and emission, respectively.

## 2.1 MADE3

MADE3 is based on MADE-in (Aquila et al., 2011), an extension of MADE as described by Lauer et al. (2005). The first generation of MADE was developed for application in a regional model (Ackermann et al., 1998). It was derived from work by Whitby et al. (1991) and Binkowski and Shankar (1995). Subsequently, MADE was adapted for global applications and implemented into the general circulation model ECHAM4 by Lauer et al. (2005), and later transformed into a submodel (Lauer et al., 2007) for the MESSy framework. The second generation submodel MADE-in was developed by Aquila et al. (2011) as an extension to the MADE version used by Lauer et al. (2007). It was created to enable simulation of number concentrations and mixing states of particles containing the insoluble components black carbon and mineral dust. For the first version of the third generation submodel MADE3, we extended the microphysical calculations to also take into account coarse particles, which were formerly regarded as passive. For version 2.0b, we also extended the gas-particle partitioning scheme. The “b” stands for beta, which we include in the version number because MADE3 has not yet been tested as part of the 3-D model. Hence, some minor changes may still be required to reach a fully operational version 2.0.

Despite substantial restructuring of the code during the development of MADE3 and the addition of new features, the third generation submodel still shares with MADE most of its features and the concepts underlying the computer code. The following sections

are meant to serve as a reference for the mathematics on which the new submodel is based.

### 2.1.1 Aerosol properties

Different numerical representations of the number distribution function  $n^*(\mu, t)$  are used in aerosol (sub)models, depending on the available computational resources, i.e. on the target application. A very accurate representation is to track particles individually, as is done in PartMC-MOSAIC (see Sect. 2.3). However, if  $N_p$  particles are tracked individually, the condensation/evaporation terms in Eq. (1), for instance, have to be calculated  $N_p$  times. To adequately represent the whole size range of atmospheric particles,  $N_p$  has to be on the order of  $10^5$ . The computational cost of such an approach would be prohibitive for application in an AC-GCM such as EMAC. Therefore, the number distribution  $n^*(\mu, t)$  is represented in MADE3 in a simplified manner, namely using the so-called modal approach. Instead of individual particle component masses, the characteristic variable is taken to be particle diameter, and the number distribution is approximated by a superposition of nine modes, i.e. nine lognormal functions  $n_k(\ln \tilde{D}, t)$  in diameter space ( $k = 1, \dots, 9$  is the mode index):

$$\begin{aligned}
 n(\ln \tilde{D}, t) &= \frac{\partial N(\ln \tilde{D}, t)}{\partial \ln \tilde{D}} \\
 &= \sum_{k=1}^9 n_k(\ln \tilde{D}, t) \\
 &= \sum_{k=1}^9 \frac{N_k(t)}{\sqrt{2\pi} \ln \sigma_k} e^{-\frac{[\ln \tilde{D} - \ln \tilde{D}_{g,k}(t)]^2}{2(\ln \sigma_k)^2}}
 \end{aligned} \tag{3}$$

where  $N(\ln \tilde{D}, t)$  is the cumulative number concentration of particles with diameters smaller than  $\tilde{D}$ . The tilde (as in  $\tilde{D}$ ) is used to indicate that the diameter was made

Title Page

Abstract

Introduction

Conclusions

References

Tables

Figures

◀

▶

◀

▶

Back

Close

Full Screen / Esc

Printer-friendly Version

Interactive Discussion



MADE3 – description  
and test

J. C. Kaiser et al.

Title Page

Abstract

Introduction

Conclusions

References

Tables

Figures

◀

▶

◀

▶

Back

Close

Full Screen / Esc

Printer-friendly Version

Interactive Discussion



dimensionless by division by  $1\ \mu\text{m}$ . Each mode  $k$  is described by three parameters, namely the number concentration of particles  $N_k(t)$  in that mode, its median particle diameter (geometric mean diameter)  $\tilde{D}_{g,k}(t)$ , and its width (geometric standard deviation)  $\sigma_k$ . Note that we do not write out time dependencies explicitly in the remainder of this paper. Mode widths are fixed in MADE3 (as was the case for its predecessor submodels) in order to further reduce the computational burden of the submodel. The values of  $\sigma_k$  are listed in Table 1. All particles in one mode  $k$  are assumed to have the same composition, i.e. the mass fractions  $c_{a,k} / \sum_{s=1}^A c_{s,k}$  are the same for these particles. The symbol  $c_{a,k}$  ( $c_{s,k}$ ) denotes the mass concentration of species  $a$  ( $s$ ) in mode  $k$  per unit volume of air.

Information about particle composition is lost in the size distribution representation as given by Eq. (3). Hence, we also track  $c_{a,k}$ , as described in Sect. 2.1.2. In MADE3 the number of equations to be solved is thus  $9 \times (1 + A)$ , i.e. one equation for the number concentration ( $N_k$ ) per mode and  $A$  equations for the different aerosol component species ( $c_{a,k}$ ) per mode. With  $A = 9$  species only 90 equations are required in MADE3 instead of  $N_p \sim 10^5$  in PartMC-MOSAIC to solve the aerosol dynamics equation (Eq. 1). The median diameter  $D_{g,k}$  of mode  $k$  can be derived from the component mass concentrations  $c_{a,k}$  in that mode under the assumption of spherical particles ( $\rho_a$  is the density of species  $a$ , see Table 1):

$$D_{g,k} = \left( \frac{6V_k}{\pi N_k} e^{-\frac{9}{2}(\ln \sigma_k)^2} \right)^{\frac{1}{3}} \quad (4)$$

with

$$V_k = \sum_{a=1}^A \frac{c_{a,k}}{\rho_a} \quad (5)$$

being the particle volume concentration of mode  $k$ .

Integral moments of the lognormal distribution are often used in the internal MADE3 computations to facilitate the calculations described in the following subsection. The  $j$ -th moment of mode  $k$  is defined as

$$M_{j,k} = \int_{-\infty}^{\infty} \tilde{D}^j \cdot 1 \mu m^j \cdot n_k(\ln \tilde{D}) d \ln \tilde{D} \quad (6)$$

$$= N_k \cdot (D_{g,k})^j e^{\frac{j^2}{2} (\ln \sigma_k)^2}$$

The 0-th moment is a mode's number concentration ( $N_k$ ), the second moment is related to its particle surface area concentration, and the third moment is related to the mode's particle volume concentration ( $V_k = \pi \cdot M_{3,k} / 6$ , cf. Eq. 5). These moments are used, for instance, to calculate coagulation and condensation rates (Whitby et al., 1991; Lauer et al., 2005; Aquila et al., 2011).

The nine modes in MADE3 (Fig. 1) are representative of three size ranges: the Aitken (tens of nanometers), accumulation (hundreds of nanometers), and coarse modes (micrometers). In each size range MADE3 includes one mode of fully soluble particles, one mode of insoluble particles and one mixed mode. The choice of this set of aerosol modes follows the ideas presented by Aquila et al. (2011), now extended to cover also the coarse mode size range.

Particles in MADE3 consist of up to nine different components, sometimes also called tracers, as they may represent more than one chemical species (Fig. 1, Table 1): sulfate ( $\text{SO}_4$ ), ammonium ( $\text{NH}_4$ ), nitrate ( $\text{NO}_3$ ), a tracer that contains sea spray components other than chloride (named Na), chloride (Cl), particulate organic matter (POM), black carbon (BC), mineral dust (DU), and water ( $\text{H}_2\text{O}$ ). Note that we do not add charges to the tracer names here because we do not distinguish between different oxidation and phase states of the aerosol components. For instance, the  $\text{SO}_4$  tracer includes  $\text{SO}_4^{2-}$ ,  $\text{HSO}_4^-$ , and liquid  $\text{H}_2\text{SO}_4$ , as well as the sulfate in  $(\text{NH}_4)_2\text{SO}_4$  and other crystalline salts.

Title Page

Abstract

Introduction

Conclusions

References

Tables

Figures

◀

▶

◀

▶

Back

Close

Full Screen / Esc

Printer-friendly Version

Interactive Discussion



## 2.1.2 Aerosol processes

Particle composition and number concentration undergo changes during the atmospheric processing of the aerosol. MADE3 calculates the evolution of the particle population due to three main processes: (1) gas-particle partitioning of semi-volatile species and water, which adds or removes particulate mass depending on environmental parameters (such as temperature or relative humidity); (2) gas-to-particle conversion of low-volatility species by condensation on pre-existing particles or in situ formation of new particles; (3) mass transfer between particles by coagulation, which concurrently reduces particle number concentration. Employing an operator splitting approach, MADE3 first calculates compositional changes due to gas-particle partitioning alone. Subsequently, condensation/new particle formation and coagulation are treated simultaneously.

### Gas-particle partitioning

Gas-particle partitioning of semi-volatile trace constituents ( $\text{NH}_3/\text{NH}_4$ ,  $\text{HNO}_3/\text{NO}_3$ ,  $\text{HCl}/\text{Cl}$ ) and water is calculated in MADE3 using the thermodynamic equilibrium model EQSAM (Equilibrium Simplified Aerosol Model; Metzger et al., 2002, 2006). The assumption of equilibrium between the gas and condensed phases is well justified for fine particles because they equilibrate on time scales on the order of seconds up to a few minutes (e.g. Meng and Seinfeld, 1996), i.e. well within the typical time step used for aerosol studies with EMAC ( $\sim 30$  min in T42 resolution, i.e.  $\approx 2.8^\circ \times 2.8^\circ$ ).

For coarse particles, however, gas diffusion may be too slow to enable equilibration within this time frame (e.g. Wexler and Seinfeld, 1990, 1992; Meng and Seinfeld, 1996). Hence, the equilibrium assumption may introduce substantial errors (Moya et al., 2002; Koo et al., 2003; Feng and Penner, 2007; Athanasopoulou et al., 2008), but fully dynamical calculations of the involved fluxes are infeasible in long-term simulations with AC-GCMs. Several solutions to this problem have been proposed (Capaldo et al., 2000; Pilinis et al., 2000; Jacobson, 2005; Zaveri et al., 2008). However, most of them are still

GMDD

7, 691–739, 2014

## MADE3 – description and test

J. C. Kaiser et al.

Title Page

Abstract

Introduction

Conclusions

References

Tables

Figures

◀

▶

◀

▶

Back

Close

Full Screen / Esc

Printer-friendly Version

Interactive Discussion



computationally too expensive for application in MADE3 within EMAC, and the solution by Zaveri et al. (2008) would require a complete revision of the chemistry scheme as used in previous simulations with MADE (e.g. Lauer et al., 2007; Aquila et al., 2011; Righi et al., 2011, 2013). Consequently, we account for possible non-equilibrium effects by limiting the gas-particle fluxes involving coarse particles in a similar manner as described by Pringle et al. (2010). We calculate the maximum possible diffusion fluxes of the semi-volatile gases (using equations equivalent to Eqs. (8) and (9) with  $g_{X,s} = 0$ ) and perform an equilibrium calculation with EQSAM. If the fluxes required to reach this equilibrium surpass the maximum fluxes, we limit the amount of material that condenses during one time step accordingly.

### Condensation of H<sub>2</sub>SO<sub>4</sub> and organic vapours

Condensation of H<sub>2</sub>SO<sub>4</sub> is calculated as the rate of change of the mass concentration  $c_{\text{H}_2\text{SO}_4,k}$  for each mode  $k$ :

$$\left(\frac{dc_{\text{H}_2\text{SO}_4,k}}{dt}\right)_{\text{cond}} = \int_0^{\infty} \frac{dm_p(D)}{dt} n_k(D) dD \quad (7)$$

where  $dm_p(D)/dt$  is the rate of change of mass for an individual particle of diameter  $D$  and  $n_k(D) dD = n_k(\ln \tilde{D}) d \ln \tilde{D}$  (cf. Eq. 3). The rate of particle mass change depends on the ratio of the particle diameter  $D$  to the mean free path of H<sub>2</sub>SO<sub>4</sub> molecules in the gas phase,  $\lambda$ . As atmospheric aerosol particles span a large range of sizes, two limiting cases have to be considered. In the continuum regime, i.e. for  $D \gg \lambda$ , one obtains (cf. Seinfeld and Pandis, 2006):

$$\left(\frac{dm_p(D)}{dt}\right)^{\text{cont}} = 2\pi D \Delta_{\text{H}_2\text{SO}_4} (g_{\text{H}_2\text{SO}_4,\infty} - g_{\text{H}_2\text{SO}_4,s}) \quad (8)$$

with the gas phase diffusivity  $\Delta_{\text{H}_2\text{SO}_4}$ . The additional indices “ $\infty$ ” and “s” specify gas phase concentrations far away from the particle surface and directly above it, respectively. The corresponding expression for the kinetic, or free molecular, regime where  $D \ll \lambda$  is (cf. Seinfeld and Pandis, 2006):

$$\left(\frac{dm_p(D)}{dt}\right)^{\text{free}} = \frac{\pi D^2}{4} \alpha_{\text{H}_2\text{SO}_4} \omega_{\text{H}_2\text{SO}_4} (g_{\text{H}_2\text{SO}_4, \infty} - g_{\text{H}_2\text{SO}_4, \text{s}}) \quad (9)$$

Here,  $\alpha_{\text{H}_2\text{SO}_4}$  is the accommodation coefficient (see Table 1) and  $\omega_{\text{H}_2\text{SO}_4}$  the thermal speed of the  $\text{H}_2\text{SO}_4$  molecules:

$$\omega_{\text{H}_2\text{SO}_4} = \sqrt{\frac{8RT}{\pi M_{\text{H}_2\text{SO}_4}}} \quad (10)$$

where  $R$  is the universal gas constant,  $T$  the absolute temperature, and  $M_{\text{H}_2\text{SO}_4}$  the molar mass of  $\text{H}_2\text{SO}_4$ . Note that a wide range of values for  $\alpha_{\text{H}_2\text{SO}_4}$  has been derived from measurements (0.02–0.79; e.g. Van Dingenen and Raes, 1991; Kerminen and Wexler, 1995; Jefferson et al., 1997; Bardouki et al., 2003) and used in models (0.1–1; e.g. Capaldo et al., 2000; Vignati et al., 2004; Zaveri et al., 2008; Mann et al., 2010; Kajino et al., 2012). Here, we use  $\alpha_{\text{H}_2\text{SO}_4} = 1$  as in former versions of MADE, which was also found to be in agreement with field measurements by Eisele and Tanner (1993). We set  $g_{\text{H}_2\text{SO}_4, \text{s}} = 0$  due to the very low equilibrium vapour pressure of  $\text{H}_2\text{SO}_4$ . For  $g_{\text{H}_2\text{SO}_4, \infty}$  we use the solution to the ordinary differential equation that describes the temporal evolution of the gas phase  $\text{H}_2\text{SO}_4$  concentration  $g_{\text{H}_2\text{SO}_4}$ :

$$\frac{dg_{\text{H}_2\text{SO}_4}}{dt} = P_{\text{H}_2\text{SO}_4} - L_{\text{H}_2\text{SO}_4} \cdot g_{\text{H}_2\text{SO}_4} \quad (11)$$

Here,  $P_{\text{H}_2\text{SO}_4}$  is the production rate of gaseous  $\text{H}_2\text{SO}_4$  and  $L_{\text{H}_2\text{SO}_4}$  is the sum of the integrals (Eq. 7) for all nine modes with the factor  $g_{\text{H}_2\text{SO}_4, \infty}$  removed, i.e. the overall

**MADE3 – description and test**

J. C. Kaiser et al.

Title Page

Abstract

Introduction

Conclusions

References

Tables

Figures

◀

▶

◀

▶

Back

Close

Full Screen / Esc

Printer-friendly Version

Interactive Discussion



loss coefficient due to condensation:

$$L_{\text{H}_2\text{SO}_4} = \frac{\sum_{k=1}^9 \left( \frac{dc_{\text{H}_2\text{SO}_4,k}}{dt} \right)_{\text{cond}}}{g_{\text{H}_2\text{SO}_4,\infty}} \quad (12)$$

Production of gaseous  $\text{H}_2\text{SO}_4$  and condensation on the particles are thus considered in parallel.

The integral in Eq. (7) can be evaluated analytically with both expressions for  $dm_p(D)/dt$  (Whitby et al., 1991). However, there is also a transition regime, where  $D$  and  $\lambda$  are of the same order of magnitude. We therefore apply the method of Binkowski and Shankar (1995), using half the harmonic mean of the two integrals as the condensation rate of  $\text{H}_2\text{SO}_4$  on mode  $k$ . For more details on the condensation calculations in MADE3 see the description in Appendix A of Aquila et al. (2011) or the original work by Whitby et al. (1991).

Secondary organic aerosol (SOA) formation from condensing organic vapours is treated in the same simplified manner in MADE3 as in MADE-in (Aquila et al., 2011). Using an externally supplied mass formation rate of SOA ( $P_{\text{SOA}}$ ), we apply a similar procedure as outlined above for  $\text{H}_2\text{SO}_4$  condensation. The SOA production rate is multiplied by the time step duration  $\Delta t$  to obtain  $g_{\text{SOA},\infty}$  for analogous expressions to Eqs. (8) and (9). The near-surface gas phase concentration is again set to zero ( $g_{\text{SOA},s} = 0$ , neglecting semi-volatile organic species because organic gas phase chemistry is not considered) so that the integral in Eq. (7) can be evaluated just as for  $\text{H}_2\text{SO}_4$ .

## New particle formation

Nucleation of new particles from  $\text{H}_2\text{SO}_4$  and  $\text{H}_2\text{O}$  is calculated in MADE3 after solving the production-condensation equation (Eq. 11). This approach corresponds to method 2C as discussed by Wan et al. (2013). In terms of the nucleation sink for gaseous  $\text{H}_2\text{SO}_4$ , they showed this method to be the best-performing among sequential methods for solving the full  $\text{H}_2\text{SO}_4$  equation, i.e. Eq. (11) plus a nucleation loss term.

Title Page

Abstract

Introduction

Conclusions

References

Tables

Figures

◀

▶

◀

▶

Back

Close

Full Screen / Esc

Printer-friendly Version

Interactive Discussion



To calculate the rate  $(dN_1/dt)_{\text{nuc}}$  we apply the parameterisation by Vehkamäki et al. (2002, 2013) that is based on temperature, RH, and  $\text{H}_2\text{SO}_4$  concentration. Following Binkowski and Roselle (2003), we account for rapid growth of the freshly nucleated particles to detectable sizes by assuming a monodisperse size distribution with  $D = 3.5 \text{ nm}$  upon formation. The  $\text{H}_2\text{SO}_4$  fraction of these particles is calculated from the ambient RH as described in Binkowski and Roselle (2003), based on measurements by Nair and Vohra (1975). Subsequently, their number and mass concentrations are added to the soluble Aitken mode ( $k = 1$ ). New particle formation from organic precursor gases is not considered in MADE3.

## Coagulation

Similar to the condensation treatment, coagulation calculations in MADE3 are also performed by mode. Number and mass changes are calculated separately:

$$\left(\frac{dN_k}{dt}\right)_{\text{coag}} = \sum_{l=1}^9 \sum_{m=l}^9 \left( a_{lm}^k \cdot \int_0^\infty \int_0^\infty \beta(D_1, D_2) n_l(D_1) n_m(D_2) dD_1 dD_2 \right) \quad (13)$$

$$\begin{aligned} \left(\frac{dC_{a,k}}{dt}\right)_{\text{coag}} = & \frac{\pi}{6} \cdot \sum_{l=1}^9 \sum_{m=l}^9 \left[ \left( \delta_{k,\tau_{lm}} - \delta_{k,l} \right) \cdot \frac{C_{a,l}}{\sum_{s=1}^A C_{s,l}} \right. \\ & \cdot \rho_l \cdot \int_0^\infty \int_0^\infty (D_1)^3 \beta(D_1, D_2) n_l(D_1) n_m(D_2) dD_1 dD_2 \\ & + \left( \delta_{k,\tau_{lm}} - \delta_{k,m} \right) \cdot \frac{C_{a,m}}{\sum_{s=1}^A C_{s,m}} \\ & \left. \cdot \rho_m \cdot \int_0^\infty \int_0^\infty (D_2)^3 \beta(D_1, D_2) n_l(D_1) n_m(D_2) dD_1 dD_2 \right] \quad (14) \end{aligned}$$

Title Page

Abstract

Introduction

Conclusions

References

Tables

Figures

◀

▶

◀

▶

Back

Close

Full Screen / Esc

Printer-friendly Version

Interactive Discussion



The parameters  $\rho_l$  and  $\rho_m$  in Eq. (14) stand for the densities of particles in modes  $l$  and  $m$ , respectively. The coefficients  $a_{lm}^k$  are calculated as follows:

$$a_{lm}^k = \delta_{k,\tau_{lm}} \cdot \left(1 + \frac{\delta_{l,m}}{2}\right) - \delta_{k,l} - \delta_{k,m} \quad (15)$$

5 Here, as in Eq. (14), the Kronecker symbol  $\delta_{x,y}$  has been used. Its value is  $\delta_{x,y} = 1$  if  $x = y$  and  $\delta_{x,y} = 0$  otherwise. The matrix elements  $\tau_{lm}$  are used for the assignment of particle number and mass concentrations to a target mode depending on the modes of origin  $l$  and  $m$ . For instance, if the particles that result from intermodal coagulation of particles from modes  $l = 1$  and  $m = 4$  are assigned to mode  $\tau_{14} = 4$ , then  $a_{14}^4 = 0$ .  
 10 Similarly,  $a_{11}^1 = -0.5$  if  $\tau_{11} = 1$ , in order to correct for the double integration over the same mode in case of intramodal coagulation. The rules for assignment of coagulated particles, i.e. the values of the matrix elements  $\tau_{lm}$ , follow Aquila et al. (2011):

- intramodal coagulation produces particles in the same mode ( $\tau_{ll} = l$ );
- intermodal coagulation produces particles in the size range of the larger mode;
- 15 – the exact target mode for intermodal coagulation depends on the mass fraction  $x$  of soluble material and water in the final particles:

$x = 1$ : soluble mode,

$0.1 \leq x < 1$ : mixed mode,

$x < 0.1$ : insoluble mode.

20 For the Brownian coagulation kernel  $\beta(D_1, D_2)$  we use the approximate formulations developed by Whitby et al. (1991) that can be integrated analytically. Two different expressions are required again, depending on the size of the particles. For the continuum regime the function is given as (Whitby et al., 1991):

$$\beta^{\text{cont}}(D_1, D_2) = \frac{2k_B T}{3\nu} \cdot \left[ 2 + 2\lambda A \left( \frac{1}{D_1} + \frac{D_2}{(D_1)^2} \right) + 2\lambda A \left( \frac{1}{D_2} + \frac{D_1}{(D_2)^2} \right) + \frac{D_2}{D_1} + \frac{D_1}{D_2} \right] \quad (16)$$

**MADE3 – description and test**

J. C. Kaiser et al.

Title Page	
Abstract	Introduction
Conclusions	References
Tables	Figures
◀	▶
◀	▶
Back	Close
Full Screen / Esc	
Printer-friendly Version	
Interactive Discussion	



with Boltzmann's constant  $k_B$ , atmospheric dynamic viscosity  $\nu$ , and the constant  $A = 1.246$  that accounts for the reduced drag on small particles. Atmospheric viscosity is calculated from temperature:

$$\nu = B \cdot \frac{T^{\frac{3}{2}}}{T + S} \quad (17)$$

with  $B = 1.458 \times 10^{-6} \text{ kg m}^{-1} \text{ s}^{-1} \text{ K}^{-0.5}$  and  $S = 110.4 \text{ K}$ . The mean free path depends on both temperature and pressure:

$$\lambda = \Lambda \cdot \frac{\rho_0 T}{T_0 \rho} \quad (18)$$

where  $\Lambda = 6.6328 \times 10^{-8} \text{ m}$ ,  $\rho_0 = 101\,325 \text{ Pa}$ , and  $T_0 = 288.15 \text{ K}$ . For the free molecular regime, the coagulation kernel becomes (Whitby et al., 1991):

$$\beta^{\text{free}}(D_1, D_2) = \sqrt{\frac{6k_B T}{\rho_1 + \rho_2}} \left( \sqrt{D_1} + 2 \frac{D_2}{\sqrt{D_1}} + \frac{(D_2)^2}{(D_1)^{3/2}} + \frac{(D_1)^2}{(D_2)^{3/2}} + 2 \frac{D_1}{\sqrt{D_2}} + \sqrt{D_2} \right) \quad (19)$$

where  $\rho_n$  is the density of the particle with diameter  $D_n$ . Note that a correction factor is required for the integrals in Eqs. (13) and (14) when this kernel approximation is used. It is set constant at 0.8 for unimodal and 0.9 for bimodal coagulation in the free molecular regime in MADE3. After evaluation of the coagulation integrals for both regimes (i.e. with  $\beta^{\text{cont}}(D_1, D_2)$  and  $\beta^{\text{free}}(D_1, D_2)$ , respectively) the halved harmonic means of the resulting rates are used to redistribute mass and numbers among the modes (cf. Appendix B in Aquila et al., 2011).

## Renaming

As particles grow by condensation and coagulation, the Aitken modes may grow into the size range of the accumulation modes. In order to avoid mode merging, i.e. to keep

## MADE3 – description and test

J. C. Kaiser et al.

Title Page

Abstract

Introduction

Conclusions

References

Tables

Figures

◀

▶

◀

▶

Back

Close

Full Screen / Esc

Printer-friendly Version

Interactive Discussion



**MADE3 – description  
and test**

J. C. Kaiser et al.

Title Page

Abstract

Introduction

Conclusions

References

Tables

Figures

◀

▶

◀

▶

Back

Close

Full Screen / Esc

Printer-friendly Version

Interactive Discussion



the modes approximately within their assigned size ranges, we apply a procedure that is termed renaming (Binkowski and Roselle, 2003). One of two criteria must be met to trigger renaming within a time step. Either the volume growth rate of the Aitken mode must be larger than that of the corresponding accumulation mode, or the median diameter of the Aitken mode must exceed 30 nm and its number concentration must be greater than that of the corresponding accumulation mode. In such a case the number concentration of particles greater than the intersection diameter of the two number size distributions is shifted from the Aitken to the corresponding accumulation mode. The associated mass concentration is also transferred. Renaming is performed only between modes of the same particle type, i.e. either between the two soluble modes, or between the two insoluble modes, or between the two mixed modes. Note that we do not rename particles from the accumulation to the coarse modes because their diameters are changed much less by condensation and coagulation than those of the Aitken mode particles.

**Aging of insoluble particles**

The aerosol processing in the atmosphere is also termed aging. For insoluble particles this term often refers to the acquisition of a coating of soluble components that transforms them from an initially hydrophobic state to a hydrophilic one. In MADE3 this transformation is realized by transfer of number and mass concentrations from the insoluble modes to the mixed modes. Following Aquila et al. (2011), we use a threshold wet mass concentration fraction of 10% of soluble material and water in an insoluble mode to trigger this procedure.

**2.2 MADE3 vs. MADE**

MADE is used here in the version described by Lauer et al. (2005). Although the code underwent major restructuring and was expanded for the development of MADE3 via MADE-in (Aquila et al., 2011), the new submodel still shares with MADE the

computational approaches to aerosol size distribution representation, gas-particle partitioning, H<sub>2</sub>SO<sub>4</sub> and SOA condensation, new particle formation, and coagulation. Here we therefore point out only the major physically motivated changes in MADE3 with respect to MADE.

5 The most obvious difference is in the number of modes, which was increased from three (MADE) to nine (MADE3). The representation of aerosol particles by three modes per size range allows us to model both internally mixed particles and externally mixed particle populations (cf. Aquila et al., 2011).

10 Furthermore, while particles in the MADE coarse mode are considered passive (only water uptake by coarse particles is included), they interact with both condensable trace gases and other particles in MADE3. Coarse particle composition as well as effects of the coarse mode on fine particles and the gas phase can therefore be resolved in much more detail with MADE3 than what is feasible with MADE. Note also that coarse particles in MADE are composed of sea spray, mineral dust, and water only, while  
15 MADE3 allows all aerosol components to be present in the coarse modes.

In combination with the larger number of modes the interactions of coarse particles also entail a larger number of different possible coagulation pathways: 45 in MADE3 vs. 2 in MADE. The calculations to determine target modes based on the soluble mass fraction of the coagulated particles is not necessary in MADE, while it is required for  
20 14 of the coagulation pathways in MADE3.

In addition, Cl is considered as a separate species in MADE3, whereas all sea spray components are lumped into one tracer in MADE. The explicit Cl representation enables the calculation of gas-aerosol partitioning for HCl by EQSAM, which is not considered in MADE, but is required for accurate modelling of processes in the marine  
25 boundary layer and in coastal areas.

The number of aerosol species tracers increased from 18 in MADE to 81 in MADE3 due to the larger number of modes, the inclusion of coarse particle interactions, and the inclusion of the Cl tracer. Furthermore, all species can now be present in any of the

---

**MADE3 – description and test**

---

J. C. Kaiser et al.

---

[Title Page](#)[Abstract](#)[Introduction](#)[Conclusions](#)[References](#)[Tables](#)[Figures](#)[◀](#)[▶](#)[◀](#)[▶](#)[Back](#)[Close](#)[Full Screen / Esc](#)[Printer-friendly Version](#)[Interactive Discussion](#)

nine modes, whereas some species (e.g. mineral dust) were excluded from the Aitken mode in MADE.

## 2.3 PartMC-MOSAIC

PartMC-MOSAIC is a stochastic particle-resolved aerosol model that consists of the microphysics code PartMC (Particle-resolved Monte Carlo model, Riemer et al., 2009) and the gas and condensed phase chemical solver MOSAIC (MODEL for Simulating Aerosol Interactions and Chemistry, Zaveri et al., 2008). The PartMC-MOSAIC version used for the present study (v. 2.2.1) corresponds to the detailed description in Tian et al. (2013), so that we only give a brief summary of the relevant features here.

The model solves the aerosol dynamics equation (Eq. 1) on a per-particle basis. While the size distribution is constrained in MADE3 by the assumption of lognormal modes, it can freely evolve in PartMC-MOSAIC, where  $n^*(\mu, t)$  is represented by a finite number  $N_p$  of computational particles with discrete sizes. For the present study we chose  $N_p \approx 10^5$ , as was done in previous applications of PartMC-MOSAIC (e.g. Riemer et al., 2009; Tian et al., 2013). In order to capture the large range of possible sizes and concentrations, one computational particle can represent a larger number of real particles (DeVillle et al., 2011). The number and mass weighting of these computational particles for the microphysics and chemistry calculations is performed automatically. As particles are constantly emitted but loss processes are not considered here (except for coagulation), half of the particles are randomly picked out and discarded whenever the number of computational particles exceeds twice its initial value.

Aerosol composition can be resolved into more separate species in PartMC-MOSAIC than in MADE3. Here, we use 11 tracers:  $\text{SO}_4$ ,  $\text{NH}_4$ ,  $\text{NO}_3$ , Na, Cl, organic carbon (OC), black carbon (BC), calcium (Ca), carbonate ( $\text{CO}_3$ ), other inorganic material (OIN), and  $\text{H}_2\text{O}$ .

Particle emissions and coagulation are treated stochastically in PartMC. Random samples are added at each time step such that the number of emitted particles per

## MADE3 – description and test

J. C. Kaiser et al.

Title Page

Abstract

Introduction

Conclusions

References

Tables

Figures

◀

▶

◀

▶

Back

Close

Full Screen / Esc

Printer-friendly Version

Interactive Discussion



**MADE3 – description  
and test**

J. C. Kaiser et al.

[Title Page](#)[Abstract](#)[Introduction](#)[Conclusions](#)[References](#)[Tables](#)[Figures](#)[⏪](#)[⏩](#)[◀](#)[▶](#)[Back](#)[Close](#)[Full Screen / Esc](#)[Printer-friendly Version](#)[Interactive Discussion](#)

unit time is Poisson distributed around a prescribed continuous mean emission rate. The composition and mean size distribution of these particles are also prescribed. For coagulation the maximum number of collision events during the time step is estimated and a corresponding number of candidate particle pairs is randomly selected. Subsequently, an accept-reject procedure is applied to determine whether these pairs actually coagulate. The probability for acceptance is based on the Brownian coagulation kernel.

Condensation of  $\text{H}_2\text{SO}_4$  and gas-particle partitioning of semi-volatile gases is dynamically calculated by the deterministic model MOSAIC. This is in contrast to the equilibrium assumption in MADE3, so that no special treatment of coarse particles is required here.

The validity of the PartMC microphysics routines was demonstrated by Riemer et al. (2009) and MOSAIC was shown to perform well in comparison to other aerosol chemistry codes (Zaveri et al., 2008), which included more details than the treatment in MADE3. The combined model (PartMC-MOSAIC) was successfully applied in a recent study of a ship plume (Tian et al., 2013). In summary, PartMC-MOSAIC is able to capture many more details of the aerosol evolution than MADE3 and can therefore serve as a reference for our comparison.

### 3 Test case setup

We performed test simulations with MADE3, MADE and PartMC-MOSAIC using initial conditions representative of the marine background boundary layer. The setup was designed to mimic the actual target application of MADE3, namely its use within the framework of the AC-GCM EMAC. As a first application, we plan to use MADE3 for a re-assessment of the shipping effect on the global atmospheric aerosol, because coarse particle interactions may play an important role in that context. Therefore, we added black carbon (BC) emissions, and prescribed gaseous  $\text{H}_2\text{SO}_4$  and  $\text{HNO}_3$  production rates in our test case, thus simulating an episode of heavy ship traffic.

**MADE3 – description  
and test**

J. C. Kaiser et al.

Title Page

Abstract

Introduction

Conclusions

References

Tables

Figures

◀

▶

◀

▶

Back

Close

Full Screen / Esc

Printer-friendly Version

Interactive Discussion



We simulate 24 h of aerosol processing (without transport and deposition, see Sect. 2) under constant environmental conditions, with a constant BC emission rate and constant  $\text{H}_2\text{SO}_4$  and  $\text{HNO}_3$  formation rates. This scenario can be regarded as an idealised representation of a stagnant air mass in a shipping corridor. For the time steps we chose typical (model-specific) values: 1800 s, i.e. 30 min, in MADE3 and MADE, and 1 s in PartMC-MOSAIC. Gas phase chemistry is not considered, because we want to focus on the particulate phase here.

Environmental parameters as well as initial gas and aerosol concentrations are extracted from a previous multi-year EMAC simulation using the MADE3 predecessor MADE-in (evaluated in Aquila et al., 2011). For our test case, we picked a grid box in the Indian Ocean with  $T = 286\text{ K}$ ,  $p = 1.02 \cdot 10^5\text{ Pa}$ , and  $\text{RH} = 0.771$ . The initial aerosol state (as represented in MADE3) is shown in Fig. 2.

As MADE-in represents coarse particles by only one mode, we redistributed the species mass concentrations among the MADE3 coarse modes as follows:

- sea spray: 50% to the soluble mode, 50% to the mixed mode;
- mineral dust (DU): 50% to the mixed mode, 50% to the insoluble mode;
- $\text{H}_2\text{O}$ : approximately 50% each to the soluble mode and the mixed mode and  $1.6 \times 10^{-4}\%$  to the insoluble mode (in order to keep the  $\text{H}_2\text{O}$  mass fraction of the latter below the 10% threshold upon initialisation).

Other species are not included in the initial coarse particle composition because MADE-in does not allow simulation of other components in the coarse mode. The redistribution of number concentration was derived from the mass concentrations in the coarse modes under the assumption that all three modes should initially have the same median diameter. Splitting up the MADE-in sea spray tracer, we assigned 45% of the mass concentration to the MADE3 Na tracer and 55% to the MADE3 Cl tracer. This speciation is in accordance with the assumptions in EQSAM on sea spray composition.

Transformation of the initial aerosol state to the MADE representation is straightforward: mass and number concentrations from the MADE-in Aitken modes were summed

up and assigned to the MADE Aitken mode, and the same procedure was applied to the accumulation modes. For the coarse mode, the MADE-in output could be used without modifications.

In terms of median diameters, number concentrations, and mode widths, PartMC-MOSAIC was initialised with the same modes as MADE3, translated to a population of individual particles. However, the MADE3 Na and DU tracers had to be further specified for use with PartMC-MOSAIC. Following again the sea spray composition assumptions in EQSAM, we assigned 69% of the MADE3 Na tracer mass concentration to the PartMC-MOSAIC Na tracer, 17% were added to the PartMC-MOSAIC SO<sub>4</sub> tracer, 3% to the Ca tracer, and 11% to the other inorganic material (OIN) tracer. For the speciation of the MADE3 DU tracer into PartMC-MOSAIC tracers we assumed the following mass fractions: 2% of Ca, 3% of CO<sub>3</sub>, and 95% of OIN (corresponding to 5% CaCO<sub>3</sub>, based on data in Glaccum and Prospero, 1980; Kandler et al., 2009; Scheuvs et al., 2013).

BC emissions are added to the (insoluble) Aitken and accumulation modes in MADE (MADE3), and as separate particles in PartMC-MOSAIC. Our BC emission flux (see Table 2) is based on the values for ship emissions reported in the Lamarque et al. (2010) dataset for the year 2000. We chose values from a grid box off the coast of Normandy, France, and assumed a bimodal size distribution for the emitted BC particles as used in Righi et al. (2013). SO<sub>2</sub> and NO<sub>x</sub> emission rates ( $P_{\text{SO}_2}$  and  $P_{\text{NO}_x}$ ) representative of ship exhaust were obtained from the same dataset and for the same grid box. In order to convert these emission rates to formation rates of gaseous H<sub>2</sub>SO<sub>4</sub> and HNO<sub>3</sub>, respectively, we first solved the ordinary differential equations

$$\frac{dg_i}{dt} = P_i - \frac{g_i}{\tau_i} \quad (20)$$

for  $i = \text{SO}_2$  and  $i = \text{NO}_x$ , assuming typical atmospheric lifetimes  $\tau_{\text{SO}_2} \approx 13\text{d}$  (based on data in Finlayson-Pitts and Pitts, 1999) and  $\tau_{\text{NO}_x} \approx 2\text{h}$  (Chen et al., 2005). Subsequently, we integrated the terms  $g_i/\tau_i$  over one time step to obtain the amounts of

**MADE3 – description and test**

J. C. Kaiser et al.

Title Page

Abstract

Introduction

Conclusions

References

Tables

Figures

◀

▶

◀

▶

Back

Close

Full Screen / Esc

Printer-friendly Version

Interactive Discussion



H<sub>2</sub>SO<sub>4</sub> and HNO<sub>3</sub> formed during the time step. As a last step, we divided those values by the time step duration to arrive at the linearised formation rates given in Table 2 along with the original emission rates.

New particle formation (NPF) is treated differently in MADE/MADE3 and PartMC-MOSAIC. Due to the large uncertainties associated with the choice of parameterisations, consideration of NPF would make the interpretation of the simulation results rather difficult. We therefore neglect the process here. In a sensitivity experiment we switched on the nucleation calculation in MADE and saw a NPF event after ~ 3h of simulated time. We added the number and mass size distributions of these nucleated particles as simulated by MADE to the initial aerosol state for all three (sub)models. Subsequently, we switched NPF off again and re-ran the simulations. Differences in the 24h number and mass size distributions were negligible for all (sub)models. Hence, we can assume that the atmospheric processing of nucleated particles is adequately treated by MADE3, i.e. growth by condensation and removal by coagulation with larger particles are properly represented.

Since some processes are treated by stochastic approaches in PartMC-MOSAIC we ran the model ten times and calculated the average of the aerosol mass and number concentrations for the ensemble of simulations. This procedure ensures that we do not discuss an “outlier” here and enables us to quantify uncertainties.

## 4 Results and discussion

### 4.1 Comparison of MADE3 and MADE

#### 4.1.1 Size distributions

Number and dry mass size distributions in MADE3 and MADE at the beginning and at the end of the 24 h simulation are plotted vs. dry diameter in Fig. 3. Dry quantities are calculated from all aerosol components except water. Although aerosol water makes

## MADE3 – description and test

J. C. Kaiser et al.

Title Page

Abstract

Introduction

Conclusions

References

Tables

Figures

⏪

⏩

◀

▶

Back

Close

Full Screen / Esc

Printer-friendly Version

Interactive Discussion



up the largest fraction of aerosol mass (see Fig. 4) we chose the dry representation here because the large H<sub>2</sub>O mass masks finer features in the size distribution. As aerosol water content is diagnosed from the composition of the dry aerosol anyway, no essential information is lost from the size distributions when neglecting H<sub>2</sub>O here.

Deviations in the size distributions after 24h in Fig. 3 are small and can be explained by the new features of MADE3 as follows.

In the fine particle size range we see a bimodal shape of the 24h MADE number size distribution which is not visible in the corresponding MADE3 distribution. This difference is due to different overlaps of the initial Aitken and accumulation modes in the two submodels, which leads to a stronger convergence of median mode diameters in MADE3 than in MADE. For the initial MADE Aitken (accumulation) mode, we summed up species mass and number concentrations of the initial MADE3 Aitken (accumulation) modes. The associated mixing of particles in MADE leads to greater median diameters for both modes with respect to the median diameters of the soluble Aitken and accumulation modes in MADE3. These soluble modes overlap more strongly during the first hours of the simulation than the Aitken and the accumulation mode in MADE. Hence, more particles are renamed from the Aitken mode to the accumulation mode in MADE3 and the accumulation mode is thus shifted towards smaller diameters. The renaming stops when the number concentration of accumulation mode particles surpasses that of the Aitken mode. This happens after about 14h and after about 18h of simulated time in MADE3 and MADE, respectively. Subsequently, the Aitken mode particles grow towards the accumulation modes by condensation. As this growth begins earlier in the MADE3 simulation than in the MADE simulation, the associated convergence of median diameters is more pronounced there.

In the coarse mode size range the difference in the 24h mass size distributions is due to the inclusion of the HCl/Cl equilibrium in MADE3. As we initialize the gas phase without HCl, equilibration requires that some of the Cl initially evaporates from the particles (see Fig. 4). This reduction in Cl is responsible for the the coarse particles' mass loss in MADE3 with respect to MADE.

**MADE3 – description and test**

J. C. Kaiser et al.

Title Page

Abstract

Introduction

Conclusions

References

Tables

Figures

⏪

⏩

◀

▶

Back

Close

Full Screen / Esc

Printer-friendly Version

Interactive Discussion



## 4.1.2 Composition

The temporal evolution of total aerosol species mass concentrations in MADE3 and MADE is plotted in Fig. 4. In both MADE3 and MADE the tracers for mineral dust (DU), black carbon (BC), particulate organic matter (POM, below  $0.001 \mu\text{g m}^{-3}$  in our marine test case), and Na (as part of the sea spray tracer in MADE) always remain in the condensed phase. Since we neglect particle sinks here, the results for these tracers are therefore identical.  $\text{SO}_4$  formation is faster in MADE3 than in MADE due to the inclusion of  $\text{H}_2\text{SO}_4$  condensation on the coarse particles. The most significant differences are seen in the  $\text{H}_2\text{O}$ , Cl,  $\text{NO}_3$ , and  $\text{NH}_4$  evolutions, where the Cl deviation was already described in the previous section and the loss of  $\text{H}_2\text{O}$  in MADE3 is due to the loss of Cl.

The  $\text{NH}_4$  uptake in MADE3 in the beginning of the simulation is coupled to  $\text{SO}_4$  uptake into the soluble Aitken mode particles. This process also occurs in the soluble accumulation mode, but only after  $\text{NaNO}_3$  has been completely displaced by  $\text{Na}_2\text{SO}_4$  ( $\sim 600$  min; note that no Na is present in the Aitken modes in our test case). In EQSAM sodium ions and sulfate are neutralised first.  $\text{NO}_3$  therefore evaporates from the soluble accumulation mode particles because of the condensation of  $\text{H}_2\text{SO}_4$  and subsequent replacement of  $\text{NaNO}_3$  by  $\text{Na}_2\text{SO}_4$ . When sulfate can no longer be neutralised by  $\text{Na}_2\text{SO}_4$  formation alone it becomes available for neutralisation by ammonium, leading to uptake of the latter into the particles. This transition is visible as the kink in the MADE3  $\text{NH}_4$  curve ( $\sim 600$  min). The same applies to the MADE Aitken and accumulation modes (see kink at  $\sim 300$  min) but proceeds faster because coarse particles are not a sink for the semi-volatile gases in MADE. This missing sink is also the reason for the second kink in the MADE  $\text{NH}_4$  evolution. As all the  $\text{H}_2\text{SO}_4$  condenses on the fine particles in MADE, they eventually enter the sulfate rich regime ( $\sim 1050$  min). From this point on, sulfate ions can bind less ammonium ions because EQSAM then assumes that sulfate exists in the forms of  $(\text{NH}_4)_2\text{SO}_4$ ,  $(\text{NH}_4)_3\text{H}(\text{SO}_4)_2$ , and  $\text{NH}_4\text{HSO}_4$  in the

Title Page

Abstract

Introduction

Conclusions

References

Tables

Figures

◀

▶

◀

▶

Back

Close

Full Screen / Esc

Printer-friendly Version

Interactive Discussion



aerosol, whereas only  $(\text{NH}_4)_2\text{SO}_4$  is considered in the sulfate neutral and sulfate poor regimes.

$\text{NO}_3$  is taken up by the coarse sea spray particles in MADE3 via  $\text{NaNO}_3$  formation despite the loss from the soluble accumulation mode. MADE, however, cannot represent this process because it considers coarse particles as passive and only a small amount of sea spray is present in the accumulation mode size range in our simulations. Hence, we see a continued increase in aerosol  $\text{NO}_3$  content for MADE3, whereas this component is completely removed from the MADE aerosol.

## 4.2 Comparison of MADE3 and PartMC-MOSAIC

### 4.2.1 Size distributions

In analogy to Sect. 4.1.1, we first compare the size distributions calculated by MADE3 and PartMC-MOSAIC (Fig. 5). Note that the PartMC-MOSAIC results are averaged over ten runs, but the variability is less than the size of the crosses in the figure. Only at the large-diameter and small-diameter limits of the size distributions as shown here, the variability is higher because of very few available computational particles.

In the coarse mode size range ( $\gtrsim 2 \mu\text{m}$ ) the 24 h distributions of the two models agree very well. The disagreement between MADE3 and PartMC-MOSAIC in the Aitken mode size range exposes a weakness of the modal approach with fixed mode widths. The Aitken mode becomes very narrow over the course of the PartMC-MOSAIC simulation. However, such narrowing cannot be simulated by MADE3, as the widths of its modes remain constant. The fast growth of the smallest particles (and slower growth of the larger Aitken mode particles) by condensation, for instance, can thus not be captured as accurately in MADE3. The 24 h MADE3 size distribution therefore contains more particles of very small diameters than the corresponding PartMC-MOSAIC distribution.

Furthermore, although total number and mass concentrations of freshly emitted BC particles are the same in both models, the size distributions upon emission are different.

## MADE3 – description and test

J. C. Kaiser et al.

Title Page

Abstract

Introduction

Conclusions

References

Tables

Figures

◀

▶

◀

▶

Back

Close

Full Screen / Esc

Printer-friendly Version

Interactive Discussion





**MADE3 – description  
and test**

J. C. Kaiser et al.

[Title Page](#)[Abstract](#)[Introduction](#)[Conclusions](#)[References](#)[Tables](#)[Figures](#)[◀](#)[▶](#)[◀](#)[▶](#)[Back](#)[Close](#)[Full Screen / Esc](#)[Printer-friendly Version](#)[Interactive Discussion](#)

achieved only after inclusion of the HCl/Cl equilibrium in EQSAM, which leads to the decrease in Cl concentration and to the associated reduction of aerosol water content as described in Sects. 4.1.1 and 4.1.2. The difference in the mineral dust (DU) concentration is due to the very low number concentration of dust containing particles. The stochastic nature of PartMC-MOSAIC thus leads to a relatively large spread of the DU concentrations in the ten simulations (not shown). Since the MADE3 result falls within the range of simulated values this deviation does not impair the overall agreement.

NO<sub>3</sub> is taken up more quickly in MADE3 than in PartMC-MOSAIC due to the assumption that equilibrium is attained during each time step. Note that the flux limit described in Sect. 2.1.2 under “Gas-particle partitioning” is never reached in our test case. In addition, there is more NO<sub>3</sub> partitioning to the condensed phase in MADE3 as it displaces Cl from the particles, leading to a slightly lower Cl content of the MADE3 aerosol. These differences can be explained by the different chemistry codes. While MOSAIC allows for coexistence of NaCl and NaNO<sub>3</sub> at arbitrary Na concentrations, NaCl can exist in EQSAM only when all the available nitrate has been bound to the sodium ions.

SO<sub>4</sub> uptake is slightly slower in PartMC-MOSAIC than in MADE3. As H<sub>2</sub>SO<sub>4</sub> condensation is limited by gas phase diffusion, the difference is due to the different assumptions for the accommodation coefficient:  $\alpha_{\text{H}_2\text{SO}_4} = 1$  in MADE3,  $\alpha_{\text{H}_2\text{SO}_4} = 0.1$  in PartMC-MOSAIC. Hence, the H<sub>2</sub>SO<sub>4</sub> flux to the particles is greater in MADE3 than in PartMC-MOSAIC (see Eq. 9). This was confirmed by a sensitivity simulation, in which we set  $\alpha_{\text{H}_2\text{SO}_4} = 0.1$  in MADE3.

The only qualitative difference between the two models in terms of composition evolution is in the NH<sub>4</sub> concentration. It is due to the different treatments of activity coefficients by EQSAM and MOSAIC (for details, see Metzger et al., 2002; Zaveri et al., 2005b). While the activity coefficient in MOSAIC allows some condensed phase NH<sub>4</sub>Cl to be produced in the accumulation mode size range, EQSAM predicts that this compound will not form in our test case.



prediction of CCN concentrations and aerosol optical depth calculations. Total aerosol mass concentrations may also differ whenever sea spray particles dominate the aerosol mass concentration.

Comparing MADE3 to PartMC-MOSAIC, we found good agreement in terms of total aerosol composition evolution and coarse particle size distribution predictions, despite some potentially significant differences in the size distributions of fine particles. It is important to note that the particle size distribution is one of the main factors that govern the conversion of aerosol particles to cloud droplets. In our test case, MADE3 results show a particularly large deviation from the PartMC-MOSAIC results in the size range where this activation primarily takes place. We will therefore have to be careful when interpreting CCN calculations in 3-D model applications of MADE3.

Nevertheless, since MADE has been extensively and successfully evaluated as part of different AC-GCMs and chemistry transport models (e.g. Lauer et al., 2005; Ochoa et al., 2012; Zhao et al., 2013; Righi et al., 2013), we are confident that MADE3 is also suitable for use with EMAC. Considering the similar results obtained for MADE3 and MADE in the box model test case that was drawn from an actual 3-D model run, we expect similar performance for MADE3 in the 3-D model as well. From the comparison with PartMC-MOSAIC we conclude that improvements in the representation of coarse aerosol particles and total aerosol composition are likely when switching from MADE to MADE3. A corresponding evaluation within the MESSy framework by means of comparison with observational data will be the subject of a follow-up study.

## 6 Code availability

The Modular Earth Submodel System (MESSy) is continuously further developed and applied by a consortium of institutions. The usage of MESSy, including MADE3, and access to the source code is licensed to all affiliates of institutions which are members of the MESSy Consortium. Institutions can become members of the MESSy Consortium

### MADE3 – description and test

J. C. Kaiser et al.

Title Page

Abstract

Introduction

Conclusions

References

Tables

Figures

⏪

⏩

◀

▶

Back

Close

Full Screen / Esc

Printer-friendly Version

Interactive Discussion





ERC grant agreement no. 226144. The aerosol model MADE was originally developed by the University of Cologne, Germany (RIU/EURAD project).

The service charges for this open access publication  
5 have been covered by a Research Centre of the  
Helmholtz Association.

## References

- Ackermann, I. J., Hass, H., Memmesheimer, M., Ebel, A., Binkowski, F. S., and Shankar, U.:  
10 Modal aerosol dynamics model for Europe: development and first applications, *Atmos. Environ.*, 32, 2981–2999, doi:10.1016/S1352-2310(98)00006-5, 1998. 694, 697, 720
- Aquila, V., Hendricks, J., Lauer, A., Riemer, N., Vogel, H., Baumgardner, D., Minikin, A., Petzold, A., Schwarz, J. P., Spackman, J. R., Weinzierl, B., Righi, M., and Dall'Amico, M.: MADE-  
15 in: a new aerosol microphysics submodel for global simulation of insoluble particles and their  
mixing state, *Geosci. Model Dev.*, 4, 325–355, doi:10.5194/gmd-4-325-2011, 2011. 694,  
697, 700, 702, 704, 706, 707, 708, 709, 712, 720
- Athanasopoulou, E., Tombrou, M., Pandis, S. N., and Russell, A. G.: The role of sea-salt emissions and heterogeneous chemistry in the air quality of polluted coastal areas, *Atmos. Chem. Phys.*, 8, 5755–5769, doi:10.5194/acp-8-5755-2008, 2008. 701
- Bardouki, H., Berresheim, H., Vrekoussis, M., Sciare, J., Kouvarakis, G., Oikonomou, K.,  
20 Schneider, J., and Mihalopoulos, N.: Gaseous (DMS, MSA, SO<sub>2</sub>, H<sub>2</sub>SO<sub>4</sub> and DMSO) and  
particulate (sulfate and methanesulfonate) sulfur species over the northeastern coast of  
Crete, *Atmos. Chem. Phys.*, 3, 1871–1886, doi:10.5194/acp-3-1871-2003, 2003. 703
- Bellouin, N., Rae, J., Jones, A., Johnson, C., Haywood, J., and Boucher, O.: Aerosol forcing in the Climate Model Intercomparison Project (CMIP5) simulations by HadGEM2-  
25 ES and the role of ammonium nitrate, *J. Geophys. Res.-Atmos.*, 116, D20206,  
doi:10.1029/2011JD016074, 2011. 693
- Bellouin, N., Quaas, J., Morcrette, J.-J., and Boucher, O.: Estimates of aerosol radiative forcing from the MACC re-analysis, *Atmos. Chem. Phys.*, 13, 2045–2062, doi:10.5194/acp-13-2045-2013, 2013. 693

## MADE3 – description and test

J. C. Kaiser et al.

Title Page

Abstract

Introduction

Conclusions

References

Tables

Figures

◀

▶

◀

▶

Back

Close

Full Screen / Esc

Printer-friendly Version

Interactive Discussion



**MADE3 – description  
and test**

J. C. Kaiser et al.

Title Page

Abstract

Introduction

Conclusions

References

Tables

Figures

◀

▶

◀

▶

Back

Close

Full Screen / Esc

Printer-friendly Version

Interactive Discussion



- Binkowski, F. S. and Roselle, S. J.: Models-3 community multiscale air quality (CMAQ) model aerosol component – 1. Model description, *J. Geophys. Res.-Atmos.*, 108, 4183, doi:10.1029/2001JD001409, 2003. 705, 708
- 5 Binkowski, F. S. and Shankar, U.: The Regional Particulate Matter Model: 1. Model description and preliminary results, *J. Geophys. Res.-Atmos.*, 100, 26191–26209, doi:10.1029/95JD02093, 1995. 697, 704
- Capaldo, K. P., Pilinis, C., and Pandis, S. N.: A computationally efficient hybrid approach for dynamic gas/aerosol transfer in air quality models, *Atmos. Environ.*, 34, 3617–3627, 2000. 701, 703
- 10 Cavalli, F., Facchini, M. C., Decesari, S., Mircea, M., Emblico, L., Fuzzi, S., Ceburnis, D., Yoon, Y. J., O'Dowd, C. D., Putaud, J.-P., and Dell'Acqua, A.: Advances in characterization of size-resolved organic matter in marine aerosol over the North Atlantic, *J. Geophys. Res.*, 109, D24215, doi:10.1029/2004JD005137, 2004. 693
- Chen, G., Huey, L. G., Trainer, M., Nicks, D., Corbett, J., Ryerson, T., Parrish, D., Neuman, J. A.,  
15 Nowak, J., Tanner, D., Holloway, J., Brock, C., Crawford, J., Olson, J. R., Sullivan, A., Weber, R., Schauffler, S., Donnelly, S., Atlas, E., Roberts, J., Flocke, F., Hübler, G., and Fehsenfeld, F.: An investigation of the chemistry of ship emission plumes during ITCT 2002, *J. Geophys. Res.-Atmos.*, 110, D10S90, doi:10.1029/2004JD005236, 2005. 713
- DeVilje, R., Riemer, N., and West, M.: Weighted Flow Algorithms (WFA) for stochastic particle  
20 coagulation, *J. Comput. Phys.*, 230, 8427–8451, doi:10.1016/j.jcp.2011.07.027, 2011. 710
- Eisele, F. L. and Tanner, D. J.: Measurement of the gas phase concentration of  $\text{H}_2\text{SO}_4$  and methane sulfonic acid and estimates of  $\text{H}_2\text{SO}_4$  production and loss in the atmosphere, *J. Geophys. Res.-Atmos.*, 98, 9001–9010, doi:10.1029/93JD00031, 1993. 703
- Feng, Y. and Penner, J. E.: Global modeling of nitrate and ammonium: Interaction of aerosols and tropospheric chemistry, *J. Geophys. Res.-Atmos.*, 112, D01304,  
25 doi:10.1029/2005JD006404, 2007. 701
- Finlayson-Pitts, B. and Pitts, J.: *Chemistry of the Upper and Lower Atmosphere: Theory, Experiments, and Applications*, Elsevier Science, 1999. 713
- Forster, P., Ramaswamy, V., Artaxo, P., Berntsen, T., Betts, R., Fahey, D., Haywood, J., Lean, J.,  
30 Lowe, D., Myhre, G., Nganga, J., Prinn, R., Raga, G., Schulz, M., and Van Dorland, R.: Changes in atmospheric constituents and in radiative forcing, in: *Climate Change 2007: The Physical Science Basis. Contribution of Working Group I to the Fourth Assessment Report of the Intergovernmental Panel on Climate Change*, edited by: Solomon, S., Qin, D., Man-

**MADE3 – description  
and test**

J. C. Kaiser et al.

Title Page

Abstract

Introduction

Conclusions

References

Tables

Figures

◀

▶

◀

▶

Back

Close

Full Screen / Esc

Printer-friendly Version

Interactive Discussion



ning, M., Chen, Z., Marquis, M., Averyt, K., Tignor, M., and Miller, H., Cambridge University Press, Cambridge, UK and New York, NY, USA, 2007. 693

Glaccum, R. A. and Prospero, J. M.: Saharan aerosols over the tropical North Atlantic – mineralogy, *Mar. Geol.*, 37, 295–321, doi:10.1016/0025-3227(80)90107-3, 1980. 713

5 Hara, K., Osada, K., Hayashi, M., Matsunaga, K., Shibata, T., Iwasaka, Y., and Furuya, K.: Fractionation of inorganic nitrates in winter Arctic troposphere: coarse aerosol particles containing inorganic nitrates, *J. Geophys. Res.-Atmos.*, 104, 23671–23679, doi:10.1029/1999JD900348, 1999. 693

10 IMO: MARPOL Consolidated Edition 2011: Articles, Protocols, Annexes, Unified Interpretations of the International Convention for the Prevention of Pollution from Ships, 1973, as Modified by the 1978 and 1997 Protocols, IMO Publication, International Maritime Organization, 2011. 693

Jacobson, M. Z.: A solution to the problem of nonequilibrium acid/base gas-particle transfer at long time step, *Aerosol Sci. Tech.*, 39, 92–103, doi:10.1080/027868290904546, 2005. 701

15 Jefferson, A., Eisele, F. L., Ziemann, P. J., Weber, R. J., Marti, J. J., and McMurry, P. H.: Measurements of the  $\text{H}_2\text{SO}_4$  mass accommodation coefficient onto polydisperse aerosol, *J. Geophys. Res.-Atmos.*, 102, 19021–19028, doi:10.1029/97JD01152, 1997. 703

Jöckel, P., Sander, R., Kerkweg, A., Tost, H., and Lelieveld, J.: Technical Note: The Modular Earth Submodel System (MESSy) - a new approach towards Earth System Modeling, *Atmos. Chem. Phys.*, 5, 433–444, doi:10.5194/acp-5-433-2005, 2005. 694

20 Jöckel, P., Kerkweg, A., Pozzer, A., Sander, R., Tost, H., Riede, H., Baumgaertner, A., Gromov, S., and Kern, B.: Development cycle 2 of the Modular Earth Submodel System (MESSy2), *Geosci. Model Dev.*, 3, 717–752, doi:10.5194/gmd-3-717-2010, 2010. 694

Johansson, L., Jalkanen, J.-P., Kalli, J., and Kukkonen, J.: The evolution of shipping emissions and the costs of regulation changes in the northern EU area, *Atmos. Chem. Phys.*, 13, 11375–11389, doi:10.5194/acp-13-11375-2013, 2013. 693

25 Kajino, M., Inomata, Y., Sato, K., Ueda, H., Han, Z., An, J., Katata, G., Deushi, M., Maki, T., Oshima, N., Kurokawa, J., Ohara, T., Takami, A., and Hatakeyama, S.: Development of the RAQM2 aerosol chemical transport model and predictions of the Northeast Asian aerosol mass, size, chemistry, and mixing type, *Atmos. Chem. Phys.*, 12, 11833–11856, doi:10.5194/acp-12-11833-2012, 2012. 703

30 Kandler, K., Schütz, L., Deutscher, C., Ebert, M., Hofmann, H., Jäckel, S., Jaenicke, R., Knipfertz, P., Lieke, K., Massling, A., Petzold, A., Schladitz, A., Weinzierl, B., Wiedensohler, A.,

**MADE3 – description  
and test**

J. C. Kaiser et al.

Title Page

Abstract

Introduction

Conclusions

References

Tables

Figures

◀

▶

◀

▶

Back

Close

Full Screen / Esc

Printer-friendly Version

Interactive Discussion



Zorn, S., and Weinbruch, S.: Size distribution, mass concentration, chemical and mineralogical composition and derived optical parameters of the boundary layer aerosol at Tinfou, Morocco, during SAMUM 200, *Tellus B*, 61, 32–50, doi:10.1111/j.1600-0889.2008.00385.x, 2009. 713

5 Kerminen, V.-M. and Wexler, A. S.: Enhanced formation and development of sulfate particles due to marine boundary layer circulation, *J. Geophys. Res.-Atmos.*, 100, 23051–23062, doi:10.1029/95JD02365, 1995. 703

Kerminen, V. M., Pakkanen, T. A., and Hillamo, R. E.: Interactions between inorganic trace gases and supermicrometer particles at a coastal site, *Atmos. Environ.*, 31, 2753–2765, doi:10.1016/S1352-2310(97)00092-7, 1997. 693

10 Koo, B., Gaydos, T. M., and Pandis, S. N.: Evaluation of the equilibrium, dynamic, and hybrid aerosol modeling approaches, *Aerosol Sci. Tech.*, 37, 53–64, doi:10.1080/02786820300893, 2003. 701

Lamarque, J.-F., Bond, T. C., Eyring, V., Granier, C., Heil, A., Klimont, Z., Lee, D., Liousse, C., Mieville, A., Owen, B., Schultz, M. G., Shindell, D., Smith, S. J., Stehfest, E., Van Aardenne, J., Cooper, O. R., Kainuma, M., Mahowald, N., McConnell, J. R., Naik, V., Riahi, K., and van Vuuren, D. P.: Historical (1850–2000) gridded anthropogenic and biomass burning emissions of reactive gases and aerosols: methodology and application, *Atmos. Chem. Phys.*, 10, 7017–7039, doi:10.5194/acp-10-7017-2010, 2010. 713

20 Lauer, A., Hendricks, J., Ackermann, I., Schell, B., Hass, H., and Metzger, S.: Simulating aerosol microphysics with the ECHAM/MADE GCM – Part I: Model description and comparison with observations, *Atmos. Chem. Phys.*, 5, 3251–3276, doi:10.5194/acp-5-3251-2005, 2005. 694, 697, 700, 708, 720, 721

Lauer, A., Eyring, V., Hendricks, J., Jöckel, P., and Lohmann, U.: Global model simulations of the impact of ocean-going ships on aerosols, clouds, and the radiation budget, *Atmos. Chem. Phys.*, 7, 5061–5079, doi:10.5194/acp-7-5061-2007, 2007. 693, 694, 697, 702

25 Lauer, A., Eyring, V., Corbett, J. J., Wang, C., and Winebrake, J. J.: Assessment of near-future policy instruments for oceangoing shipping: impact on atmospheric aerosol burdens and the Earth's radiation budget, *Environ. Sci. Technol.*, 43, 5592–5598, doi:10.1021/es900922h, 2009. 693, 694

30 Mann, G. W., Carslaw, K. S., Spracklen, D. V., Ridley, D. A., Manktelow, P. T., Chipperfield, M. P., Pickering, S. J., and Johnson, C. E.: Description and evaluation of GLOMAP-mode: a modal

**MADE3 – description  
and test**

J. C. Kaiser et al.

[Title Page](#)[Abstract](#)[Introduction](#)[Conclusions](#)[References](#)[Tables](#)[Figures](#)[◀](#)[▶](#)[◀](#)[▶](#)[Back](#)[Close](#)[Full Screen / Esc](#)[Printer-friendly Version](#)[Interactive Discussion](#)

global aerosol microphysics model for the UKCA composition-climate model, *Geosci. Model Dev.*, 3, 519–551, doi:10.5194/gmd-3-519-2010, 2010. 703

Meng, Z. Y. and Seinfeld, J. H.: Time scales to achieve atmospheric gas-aerosol equilibrium for volatile species, *Atmos. Environ.*, 30, 2889–2900, doi:10.1016/1352-2310(95)00493-9, 1996. 701

Metzger, S., Dentener, F., Pandis, S., and Lelieveld, J.: Gas/aerosol partitioning: 1. A computationally efficient model, *J. Geophys. Res.-Atmos.*, 107, ACH16.1–ACH16.24, doi:10.1029/2001JD001102, 2002. 701, 719

Metzger, S., Mihalopoulos, N., and Lelieveld, J.: Importance of mineral cations and organics in gas-aerosol partitioning of reactive nitrogen compounds: case study based on MINOS results, *Atmos. Chem. Phys.*, 6, 2549–2567, doi:10.5194/acp-6-2549-2006, 2006. 701

Moya, M., Pandis, S. N., and Jacobson, M. Z.: Is the size distribution of urban aerosols determined by thermodynamic equilibrium? An application to Southern California, *Atmos. Environ.*, 36, 2349–2365, doi:10.1016/S1352-2310(01)00549-0, 2002. 701

Naik, V., Horowitz, L. W., Fiore, A. M., Ginoux, P., Mao, J., Aghedo, A. M., and Levy, H.: Impact of preindustrial to present-day changes in short-lived pollutant emissions on atmospheric composition and climate forcing, *J. Geophys. Res.-Atmos.*, 118, 8086–8110, doi:10.1002/jgrd.50608, 2013. 693

Nair, P. and Vohra, K.: Growth of aqueous sulphuric acid droplets as a function of relative humidity, *J. Aerosol Sci.*, 6, 265–271, doi:10.1016/0021-8502(75)90094-4, 1975. 705

Nolte, C. G., Bhave, P. V., Arnold, J. R., Dennis, R. L., Zhang, K. M., and Wexler, A. S.: Modeling urban and regional aerosols – application of the CMAQ-UCD Aerosol Model to Tampa, a coastal urban site, *Atmos. Environ.*, 42, 3179–3191, doi:10.1016/j.atmosenv.2007.12.059, 2008. 693

Ochoa, C., Baumgardner, D., Grutter, M., Allan, J., Fast, J., and Rappenglueck, B.: Physical and chemical properties of the regional mixed layer of Mexico's Megapolis Part II: evaluation of measured and modeled trace gases and particle size distributions, *Atmos. Chem. Phys.*, 12, 10161–10179, doi:10.5194/acp-12-10161-2012, 2012. 721

Olivié, D. J. L., Cariolle, D., Teyssèdre, H., Salas, D., Voldoire, A., Clark, H., Saint-Martin, D., Michou, M., Karcher, F., Balkanski, Y., Gauss, M., Dessens, O., Koffi, B., and Sausen, R.: Modeling the climate impact of road transport, maritime shipping and aviation over the period 1860–2100 with an AOGCM, *Atmos. Chem. Phys.*, 12, 1449–1480, doi:10.5194/acp-12-1449-2012, 2012. 693

**MADE3 – description  
and test**

J. C. Kaiser et al.

[Title Page](#)[Abstract](#)[Introduction](#)[Conclusions](#)[References](#)[Tables](#)[Figures](#)[◀](#)[▶](#)[◀](#)[▶](#)[Back](#)[Close](#)[Full Screen / Esc](#)[Printer-friendly Version](#)[Interactive Discussion](#)

Peters, K., Stier, P., Quaas, J., and Graßl, H.: Aerosol indirect effects from shipping emissions: sensitivity studies with the global aerosol-climate model ECHAM-HAM, *Atmos. Chem. Phys.*, 12, 5985–6007, doi:10.5194/acp-12-5985-2012, 2012. 693, 694

Peters, K., Stier, P., Quaas, J., and Graßl, H.: Corrigendum to “Aerosol indirect effects from shipping emissions: sensitivity studies with the global aerosol-climate model ECHAM-HAM” published in *Atmos. Chem. Phys.*, 12, 5985–6007, 2012, *Atmos. Chem. Phys.*, 13, 6429–6430, doi:10.5194/acp-13-6429-2013, 2013. 693, 694

Pilinis, C., Capaldo, K. P., Nenes, A., and Pandis, S. N.: MADM – a new multicomponent aerosol dynamics model, *Aerosol Sci. Tech.*, 32, 482–502, doi:10.1080/027868200303597, 2000. 701

Pringle, K. J., Tost, H., Message, S., Steil, B., Giannadaki, D., Nenes, A., Fountoukis, C., Stier, P., Vignati, E., and Lelieveld, J.: Description and evaluation of GMXe: a new aerosol submodel for global simulations (v1), *Geosci. Model Dev.*, 3, 391–412, doi:10.5194/gmd-3-391-2010, 2010. 702

Riemer, N., West, M., Zaveri, R. A., and Easter, R. C.: Simulating the evolution of soot mixing state with a particle-resolved aerosol model, *J. Geophys. Res.-Atmos.*, 114, D09202, doi:10.1029/2008JD011073, 2009. 694, 696, 710, 711, 720

Righi, M., Klinger, C., Eyring, V., Hendricks, J., Lauer, A., and Petzold, A.: Climate Impact of Biofuels in Shipping: Global Model Studies of the Aerosol Indirect Effect, *Environ. Sci. Technol.*, 45, 3519–3525, doi:10.1021/es1036157, 2011. 693, 694, 702

Righi, M., Hendricks, J., and Sausen, R.: The global impact of the transport sectors on atmospheric aerosol: simulations for year 2000 emissions, *Atmos. Chem. Phys.*, 13, 9939–9970, doi:10.5194/acp-13-9939-2013, 2013. 693, 694, 702, 713, 721

Roeckner, E., Brokopf, R., Esch, M., Giorgetta, M., Hagemann, S., Kornblueh, L., Manzini, E., Schlese, U., and Schulzweida, U.: Sensitivity of simulated climate to horizontal and vertical resolution in the ECHAM5 Atmosphere Model, *J. Climate*, 19, 3771–3791, doi:10.1175/JCLI3824.1, 2006. 694

Scheuvs, D., Schütz, L., Kandler, K., Ebert, M., and Weinbruch, S.: Bulk composition of Northern African dust and its source sediments – a compilation, *Earth-Sci. Rev.*, 116, 170–194, doi:10.1016/j.earscirev.2012.08.005, 2013. 713

Seinfeld, J. and Pandis, S.: *Atmospheric chemistry and physics: from air pollution to climate change*, Wiley, Hoboken, NJ, 2nd Edn., 2006. 702, 703

**MADE3 – description  
and test**

J. C. Kaiser et al.

Title Page

Abstract

Introduction

Conclusions

References

Tables

Figures

◀

▶

◀

▶

Back

Close

Full Screen / Esc

Printer-friendly Version

Interactive Discussion



Tian, J., Riemer, N., Pfaffenberger, L., Schlager, H., and Petzold, A.: Modeling the evolution of aerosol particles in a ship plume using PartMC-MOSAIC, *Atmos. Chem. Phys. Discuss.*, 13, 16733–16774, doi:10.5194/acpd-13-16733-2013, 2013. 710, 711

Van Dingenen, R. and Raes, F.: Determination of the condensation accommodation coefficient of sulfuric acid on water-sulfuric acid aerosol, *Aerosol Sci. Tech.*, 15, 93–106, doi:10.1080/02786829108959516, 1991. 703

Vehkamäki, H., Kulmala, M., Napari, I., Lehtinen, K. E. J., Timmreck, C., Noppel, M., and Laaksonen, A.: An improved parameterization for sulfuric acid-water nucleation rates for tropospheric and stratospheric conditions, *J. Geophys. Res.*, 107, 4622–4631, doi:10.1029/2002JD002184, 2002. 705

Vehkamäki, H., Kulmala, M., Napari, I., Lehtinen, K. E. J., Timmreck, C., Noppel, M., and Laaksonen, A.: Correction to “An improved parameterization for sulfuric acid/water nucleation rates for tropospheric and stratospheric conditions”, *J. Geophys. Res.-Atmos.*, 118, 9330–9330, doi:10.1002/jgrd.50603, 2013. 705

Vignati, E., Wilson, J., and Stier, P.: M7: An efficient size-resolved aerosol microphysics module for large-scale aerosol transport models, *J. Geophys. Res.*, 109, D22202, doi:10.1029/2003JD004485, 2004. 703

Wan, H., Rasch, P. J., Zhang, K., Kazil, J., and Leung, L. R.: Numerical issues associated with compensating and competing processes in climate models: an example from ECHAM-HAM, *Geosci. Model Dev.*, 6, 861–874, doi:10.5194/gmd-6-861-2013, 2013. 704

Wexler, A. S. and Seinfeld, J. H.: The distribution of ammonium salts among a size and composition dispersed aerosol, *Atmos. Environ. A-Gen.*, 24, 1231–1246, doi:10.1016/0960-1686(90)90088-5, 1990. 701

Wexler, A. S. and Seinfeld, J. H.: Analysis of aerosol ammonium nitrate: Departures from equilibrium during SCAQS, *Atmos. Environ. A-Gen.*, 26, 579–591, doi:10.1016/0960-1686(92)90171-G, 1992. 701

Whitby, E. R., McMurry, P. H., Shankar, U., and Binkowski, F. S.: Modal aerosol dynamics modeling, Tech. Rep. EPA-68-01-7365, US Environmental Protection Agency, Office of Research and Development, Atmospheric Research and Exposure Assessment Laboratory, Research Triangle Park, NC, available at: <http://nepis.epa.gov/Exe/ZyPURL.cgi?Dockey=9100J9AO.txt> (last access: 13 June 2012), 1991. 697, 700, 704, 706, 707

**MADE3 – description  
and test**

J. C. Kaiser et al.

Title Page

Abstract

Introduction

Conclusions

References

Tables

Figures

I◀

▶I

◀

▶

Back

Close

Full Screen / Esc

Printer-friendly Version

Interactive Discussion



Yeatman, S. G., Spokes, L. J., and Jickells, T. D.: Comparisons of coarse-mode aerosol nitrate and ammonium at two polluted coastal sites, *Atmos. Environ.*, 35, 1321–1335, doi:10.1016/S1352-2310(00)00452-0, 2001. 693

5 Zaveri, R. A., Easter, R. C., and Peters, L. K.: A computationally efficient Multicomponent Equilibrium Solver for Aerosols (MESA), *J. Geophys. Res.-Atmos.*, 110, D24203, doi:10.1029/2004JD005618, 2005a. 722

Zaveri, R. A., Easter, R. C., and Wexler, A. S.: A new method for multicomponent activity coefficients of electrolytes in aqueous atmospheric aerosols, *J. Geophys. Res.-Atmos.*, 110, D02201, doi:10.1029/2004JD004681, 2005b. 719

10 Zaveri, R. A., Easter, R. C., Fast, J. D., and Peters, L. K.: Model for Simulating Aerosol Interactions and Chemistry (MOSAIC), *J. Geophys. Res.-Atmos.*, 113, D13204, doi:10.1029/2007JD008782, 2008. 694, 701, 702, 703, 710, 711, 720

15 Zhao, M., Zhang, Y., Ma, W., Fu, Q., Yang, X., Li, C., Zhou, B., Yu, Q., and Chen, L.: Characteristics and ship traffic source identification of air pollutants in China's largest port, *Atmos. Environ.*, 64, 277–286, doi:10.1016/j.atmosenv.2012.10.007, 2013. 721

**Table 1.** Parameters used in MADE3: mode widths, accommodation coefficients for gas adsorption on aerosol particles, diffusivities of gases in air, and bulk aerosol component densities. Abbreviations are: SOA for secondary organic aerosol, POM for particulate organic matter, BC for black carbon, and DU for mineral dust.

	Symbol	Value	Unit
<b>Mode widths</b>			
soluble Aitken	$\sigma_1$	1.7	
mixed Aitken	$\sigma_2$	1.7	
insoluble Aitken	$\sigma_3$	1.7	
soluble accumulation	$\sigma_4$	2.0	
mixed accumulation	$\sigma_5$	2.0	
insoluble accumulation	$\sigma_6$	2.0	
soluble coarse	$\sigma_7$	2.2	
mixed coarse	$\sigma_8$	2.2	
insoluble coarse	$\sigma_9$	2.2	
<b>Component densities</b>			
SO <sub>4</sub>	$\rho_{\text{SO}_4}$	$1.8 \times 10^3$	kgm <sup>-3</sup>
NH <sub>4</sub>	$\rho_{\text{NH}_4}$	$1.8 \times 10^3$	kgm <sup>-3</sup>
NO <sub>3</sub>	$\rho_{\text{NO}_3}$	$1.8 \times 10^3$	kgm <sup>-3</sup>
Na	$\rho_{\text{Na}}$	$2.2 \times 10^3$	kgm <sup>-3</sup>
Cl	$\rho_{\text{Cl}}$	$2.2 \times 10^3$	kgm <sup>-3</sup>
POM	$\rho_{\text{POM}}$	$1.0 \times 10^3$	kgm <sup>-3</sup>
BC	$\rho_{\text{BC}}$	$2.2 \times 10^3$	kgm <sup>-3</sup>
DU	$\rho_{\text{DU}}$	$2.5 \times 10^3$	kgm <sup>-3</sup>
H <sub>2</sub> O	$\rho_{\text{H}_2\text{O}}$	$1.0 \times 10^3$	kgm <sup>-3</sup>
<b>Accommodation coefficients</b>			
H <sub>2</sub> SO <sub>4</sub>	$\alpha_{\text{H}_2\text{SO}_4}$	1.0	
NH <sub>3</sub>	$\alpha_{\text{NH}_3}$	0.1	
HNO <sub>3</sub>	$\alpha_{\text{HNO}_3}$	0.1	
HCl	$\alpha_{\text{HCl}}$	0.1	
SOA	$\alpha_{\text{SOA}}$	1.0	
<b>Gas diffusivities</b>			
H <sub>2</sub> SO <sub>4</sub>	$\Delta_{\text{H}_2\text{SO}_4}$	0.09	cm <sup>2</sup> s <sup>-1</sup>
NH <sub>3</sub>	$\Delta_{\text{NH}_3}$	0.1	cm <sup>2</sup> s <sup>-1</sup>
HNO <sub>3</sub>	$\Delta_{\text{HNO}_3}$	0.1	cm <sup>2</sup> s <sup>-1</sup>
HCl	$\Delta_{\text{HCl}}$	0.1	cm <sup>2</sup> s <sup>-1</sup>
SOA	$\Delta_{\text{SOA}}$	0.05	cm <sup>2</sup> s <sup>-1</sup>

MADE3 – description  
and test

J. C. Kaiser et al.

**Table 2.** Emission and formation rates used in the test case.

Species	mass conc. rate of change [ $\text{kg m}^{-3} \text{s}^{-1}$ ]	number conc. rate of change [ $\text{m}^{-3} \text{s}^{-1}$ ]
Aitken mode BC ( $D_g = 70 \text{ nm}$ , $\sigma = 1.45$ )	$1.9 \times 10^{-16}$	$2.6 \times 10^2$
accumulation mode BC ( $D_g = 260 \text{ nm}$ , $\sigma = 1.25$ )	$5.0 \times 10^{-17}$	2.0
$\text{SO}_2$	$1.0 \times 10^{-14}$	–
$\text{H}_2\text{SO}_4$	$1.5 \times 10^{-14}$	–
$\text{NO}_x$	$9.8 \times 10^{-15}$	–
$\text{HNO}_3$	$1.7 \times 10^{-14}$	–

Title Page

Abstract

Introduction

Conclusions

References

Tables

Figures

◀

▶

◀

▶

Back

Close

Full Screen / Esc

Printer-friendly Version

Interactive Discussion



## MADE3 – description and test

J. C. Kaiser et al.

Title Page

Abstract

Introduction

Conclusions

References

Tables

Figures

◀

▶

◀

▶

Back

Close

Full Screen / Esc

Printer-friendly Version

Interactive Discussion

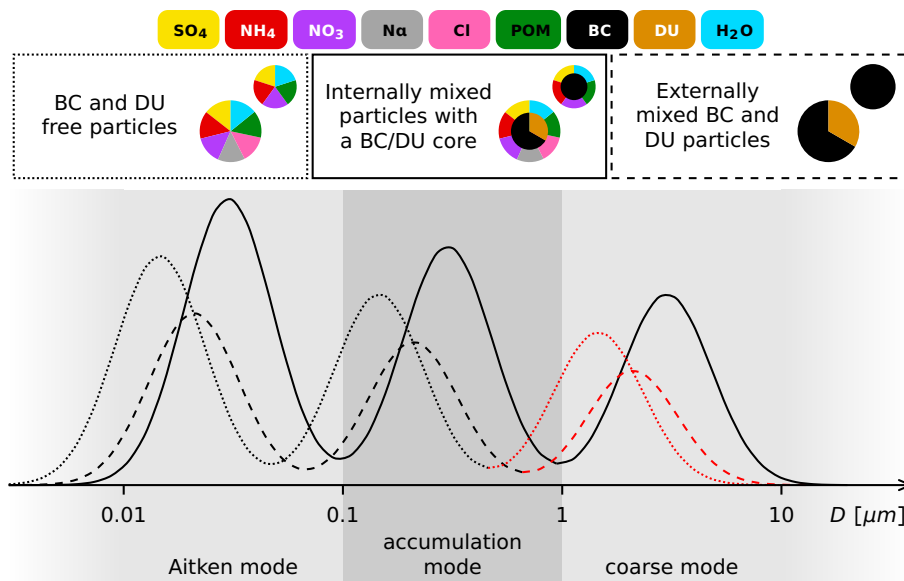


**Fig. 1.** Schematic illustration of the MADE3 modes and aerosol composition. Each size range (Aitken, accumulation, and coarse mode size range) is represented by three modes: soluble (dotted lines), insoluble (dashed lines), and mixed particles (solid lines). Red lines indicate the new contribution of MADE3 with respect to its predecessor, MADE-in. Small circles show possible Aitken mode particle compositions, larger circles stand for accumulation and coarse mode particles. Note that the MADE3 code in principle allows all components in each of the modes, but some components do not appear in significant fractions in certain types of particles in the real atmosphere (e.g. mineral dust in Aitken mode particles). Abbreviations are: POM for particulate organic matter, BC for black carbon, and DU for mineral dust.

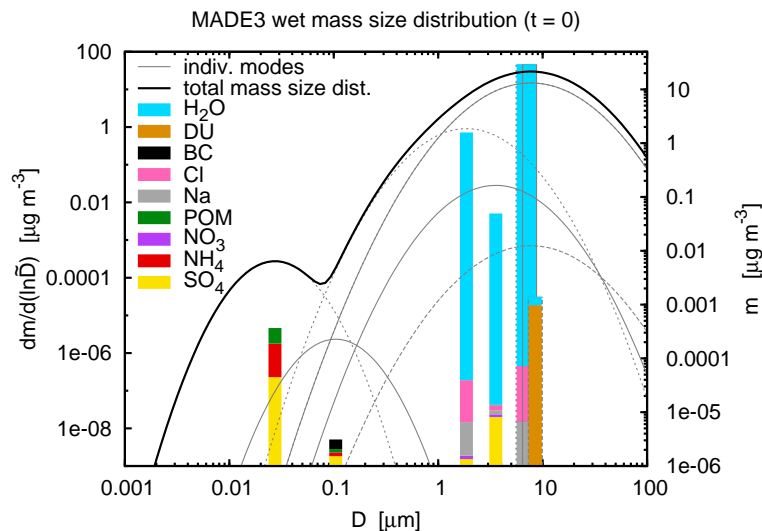


**Fig. 2.** Initial aerosol mass size distribution and composition as represented in MADE3. The thick black line represents the mass size distribution calculated as the sum of the modes shown in grey (left vertical axis; dotted lines for soluble modes, solid lines for mixed modes, dashed lines for insoluble modes). Insoluble Aitken and accumulation mode mass concentrations are initially so small that these modes do not appear in the figure, and the curves for the soluble and mixed coarse modes lie on top of each other. The coloured bars show the contributions of the individual species (POM = particulate organic matter, BC = black carbon, DU = mineral dust) to the mass concentration (right vertical axis) of the respective mode (from left to right: soluble Aitken, mixed Aitken, soluble accumulation, mixed accumulation, soluble coarse, mixed coarse, insoluble coarse). Note that while the right vertical axis is logarithmic, the species fractions in the bars add up linearly to the total masses (i.e. the axis applies only to the total masses, not to the individual contributions). Note further that the three coarse mode bars were artificially spread out along the diameter axis and grey borders corresponding to the line styles of the respective modes were added for clarity.

**MADE3 – description and test**

J. C. Kaiser et al.

Title Page

Abstract Introduction

Conclusions References

Tables Figures

◀ ▶

◀ ▶

Back Close

Full Screen / Esc

Printer-friendly Version

Interactive Discussion



MADE3 – description  
and test

J. C. Kaiser et al.

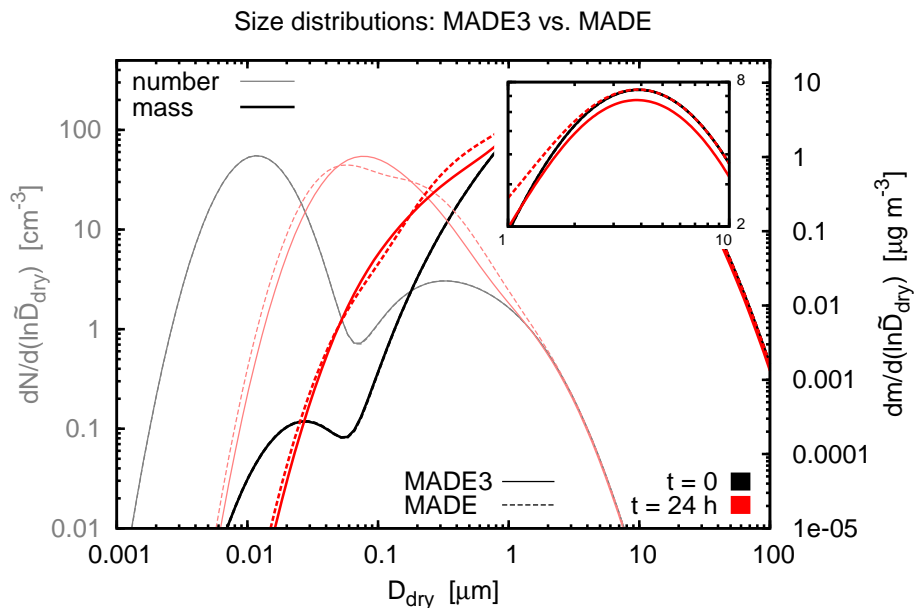


**Fig. 3.** Initial (black, grey) and final (red, light red) size distributions in MADE3 and MADE vs. dry diameter (i.e. neglecting aerosol water). Light colours (grey, light red) are used for number distributions (left vertical axis), full colours (black, red) for dry mass distributions (right vertical axis). MADE3 output is shown as solid lines, MADE output as dashed lines. The inset magnifies the coarse mode mass size distributions.

Title Page

Abstract

Introduction

Conclusions

References

Tables

Figures

◀

▶

◀

▶

Back

Close

Full Screen / Esc

Printer-friendly Version

Interactive Discussion



## MADE3 – description and test

J. C. Kaiser et al.

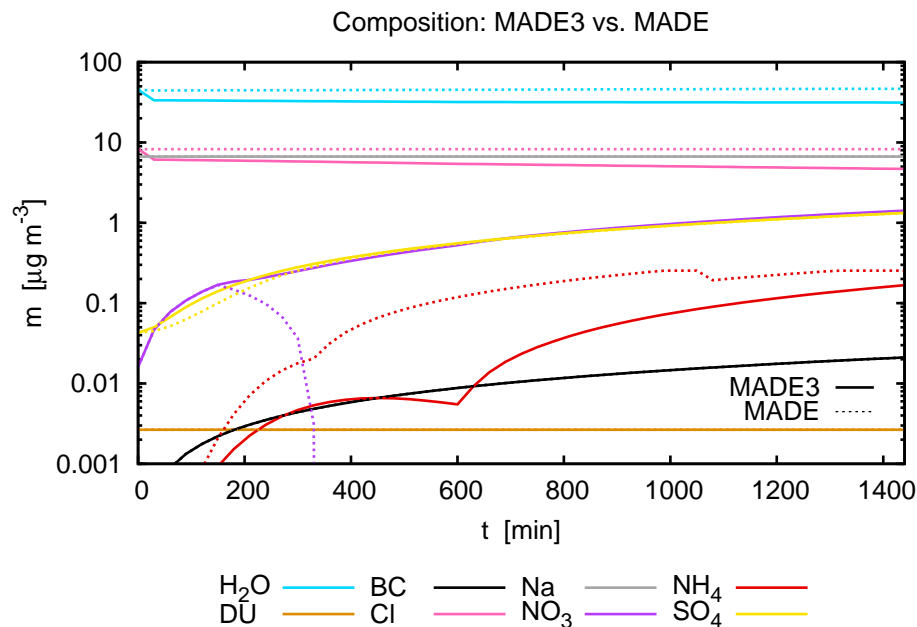


**Fig. 4.** Temporal evolution of total aerosol species mass concentrations in MADE3 (solid lines) and MADE (dotted lines). Abbreviations are: BC for black carbon and DU for mineral dust. Note that the particulate organic matter (POM) concentration is below  $0.001 \mu\text{g m}^{-3}$  and therefore does not appear in the plot.

Title Page

Abstract

Introduction

Conclusions

References

Tables

Figures

◀

▶

◀

▶

Back

Close

Full Screen / Esc

Printer-friendly Version

Interactive Discussion



MADE3 – description  
and test

J. C. Kaiser et al.

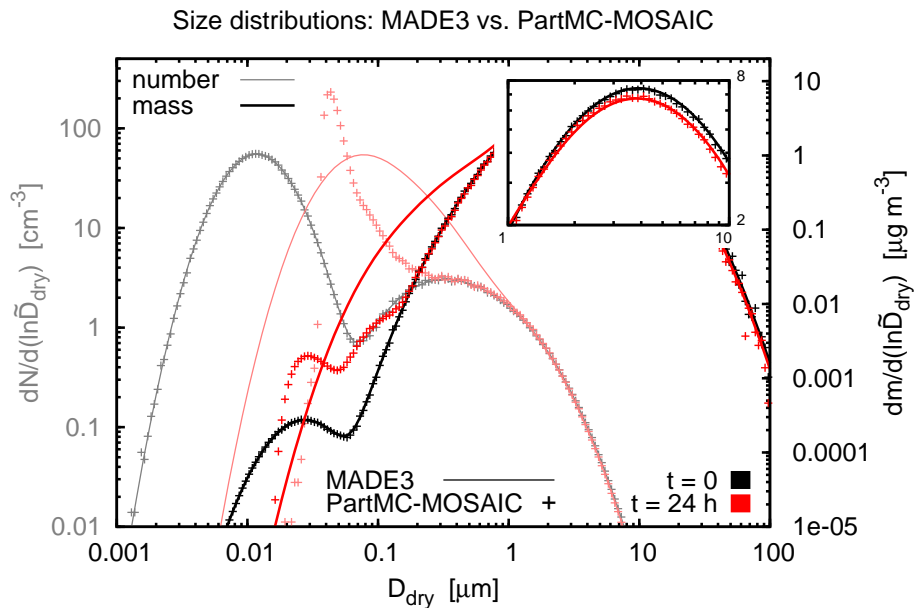


**Fig. 5.** Initial (black, grey) and final (red, light red) size distributions in MADE3 and PartMC-MOSAIC vs. dry diameter. Light colours are used for number distributions (left vertical axis), full colours for dry mass distributions (right vertical axis). MADE3 output is shown as solid lines, PartMC-MOSAIC output as crosses. The inset magnifies the coarse mode mass size distributions.

Title Page

Abstract

Introduction

Conclusions

References

Tables

Figures

◀

▶

◀

▶

Back

Close

Full Screen / Esc

Printer-friendly Version

Interactive Discussion



## MADE3 – description and test

J. C. Kaiser et al.

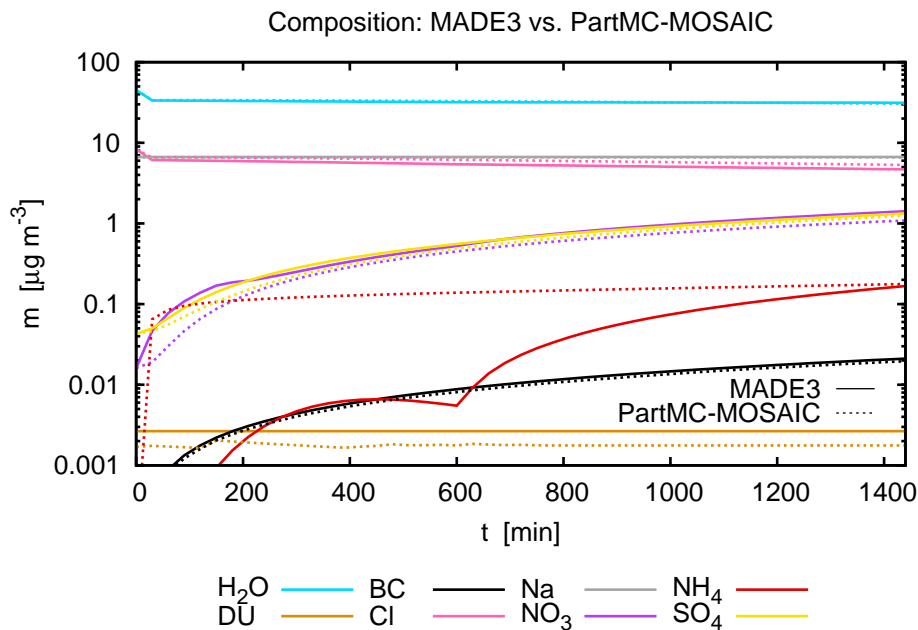


**Fig. 6.** Temporal evolution of total species mass concentrations in MADE3 (solid lines) and PartMC-MOSAIC (dotted lines). Abbreviations are: BC for black carbon and DU for mineral dust. Note that the particulate organic matter (POM) concentration is below  $0.001 \mu\text{g m}^{-3}$  and therefore does not appear in the plot.

Title Page

Abstract

Introduction

Conclusions

References

Tables

Figures

◀

▶

◀

▶

Back

Close

Full Screen / Esc

Printer-friendly Version

Interactive Discussion



## MADE3 – description and test

J. C. Kaiser et al.

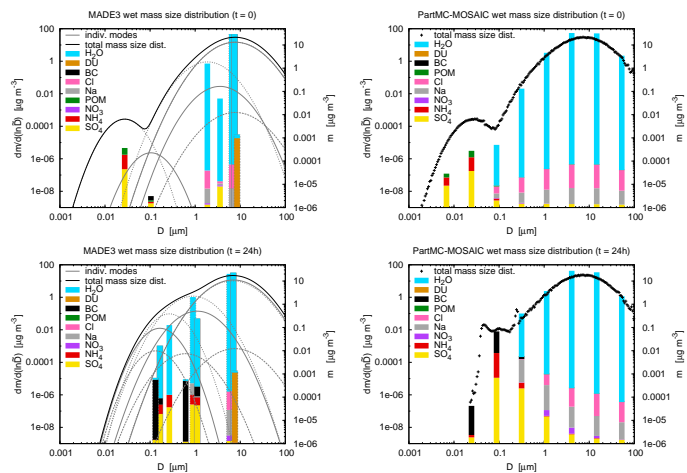


**Fig. A1.** Aerosol mass size distributions and size-resolved composition at  $t = 0$  (top panels) and  $t = 24$  h (bottom panels) for MADE3 (left panels) and PartMC-MOSAIC (right panels). In the MADE3 panels the black lines represent total mass size distributions calculated as the sums of the modes shown in grey (left vertical axes; dotted lines for soluble modes, solid lines for mixed modes, dashed lines for insoluble modes). Modes that are not shown have mass concentrations below the lower end of the scale. In the PartMC-MOSAIC panels the crosses represent total mass size distributions (left vertical axes). The coloured bars show the contributions of the individual species (POM = particulate organic matter, BC = black carbon, DU = mineral dust) to the respective mass concentration (right vertical axis). In the MADE3 plots the bars correspond to the modes, in the PartMC-MOSAIC plots particles were binned into nine size sections and the bars show the average compositions in these sections. Note that while the right vertical axis is logarithmic, the species fractions in the bars add up linearly to the total masses (i.e. the axis applies only to the total masses, not to the individual contributions). Note further that the three coarse mode bars in the MADE3 panels were spread out artificially along the diameter axis for clarity.